Bioconjugate Chemistry

Article

pubs.acs.org/bc

Preparation of Semisynthetic Lipoproteins with Fluorescent Cholesterol Anchor and Their Introduction to the Cell Membrane with Minimal Disruption of the Membrane

Balázs Schäfer,[†] Erika Orbán,[‡] Attila Borics,[†] Krisztina Huszár,[§,∥] Antal Nyeste,[§,∥] Ervin Welker,[§,∥] and Csaba Tömböly*[,†]

[†]Laboratory of Chemical Biology and [§]Laboratory of Conformational Diseases, Institute of Biochemistry, Biological Research Centre of the Hungarian Academy of Sciences, Temesvári krt. 62., 6726 Szeged, Hungary

[‡]Research Group of Peptide Chemistry, Hungarian Academy of Sciences, Pázmány Péter sétány 1/a, 1117 Budapest, Hungary

[∥]Institute of Molecular Pharmacology, Research Centre of Natural Sciences, Hungarian Academy of Sciences, Diószegi út 64., 1113 Budapest, Hungary

Supporting Information

ABSTRACT: The exogenous introduction of fluorescent lipoproteins into cell membranes is a method for visualizing the cellular traffic of membrane associated proteins, and also for altering the cell surface in a controlled manner. In order to achieve the cell membrane anchoring of proteins and their subsequent fluorescence based detection, a cholesterol derivative was designed. The headgroup of the novel cholesterol anchor contains a fluorescent reporter and a thiol reactive maleimide for protein conjugation. Protein conjugation was demonstrated by the addition of a green fluorescent maleimido anchor to the C-terminus of a Cys extended red fluorescent protein, mCherry. The resulting dual fluorescent cholesteryl lipoprotein was successfully separated from the micellar associates of the surplus fluorescent lipid anchor without denaturing the protein, and the lipoprotein containing only the covalently linked, stoichiometric fluorescent lipid was efficiently delivered to the plasma membrane of live cells. It was demonstrated that the membrane fluorescence could be directly assigned to the protein−anchor conjugate, because no excess of fluorescent lipid species were present during the imaging experiment and the protein and anchor fluorescence colocalized in the cell membrane. Molecular dynamics simulations and subsequent trajectory analysis suggest also the spontaneous and stable membrane association of the cholesterol anchor. Thus, the method could be beneficially applied for studying membrane associated proteins and for preparing mimetics of glycosylphosphatidylinositol (GPI)-anchored proteins to target cholesterol-rich membrane microdomains.

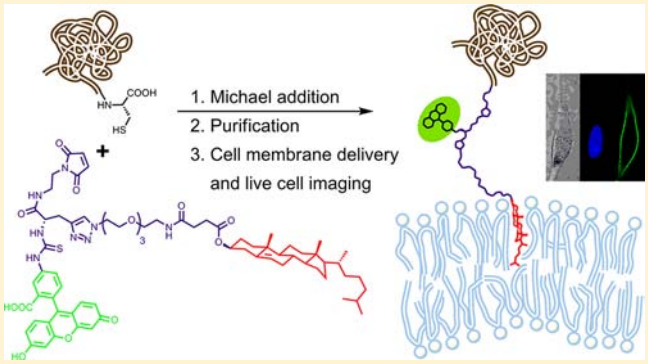

INTRODUCTION

Lipidation plays an important role in the localization and function of proteins. Four common modifications of proteins with lipid moieties are myristoylation, palmitoylation, prenylation, and the attachment of glycosylphosphatidylinositol (GPI) anchors.[1−6] The amidation of the protein C-terminus with a GPI glycolipid results in proteins tethered to the extracellular leaflet of the cell membrane.[7−9] This modification is widespread throughout eukaryotes, and more than 150 human GPI-anchored proteins (GPI-APs) are known with various functions: enzymes, receptors, complement regulation proteins, antigens, or adhesion molecules.[10] Beyond the normal physiological functions, GPI-APs are associated with a range of diseases including paroxysmal nocturnal hemoglobinuria, prion diseases, carcinogenesis, and sleeping sickness.[11−14] The important functional role of the GPI-APs is further evidenced by the embryonic lethality of the GPI-deficient mice.[15] The GPI glycolipids have the conserved Man(α1−2)Man(α1−6)Man(α1−4)GlcN(α1−6)*myo*Ino glycan core and variations arise in the substitution pattern and in the lipid composition.[10,16] The lipid part of the mammalian GPIs is phosphatidylinositol with stearyl chains; therefore, the GPI-APs are able to temporarily associate with sphingolipid- and cholesterol-rich membrane microdomains, i.e., lipid rafts.[7,16−21] This clustering is mainly due to the favorable hydrophobic interactions between the saturated acyl chains of the GPI anchor and the lipid constituents of the rafts.[7,17] It was evidenced that the lipid raft association of the GPI-APs could be abrogated by cholesterol depletion of the cell membrane and by replacing the GPI moiety with a transmembrane anchor.[22]

Received: April 24, 2013
Revised: September 4, 2013
Published: September 10, 2013

dx.doi.org/10.1021/bc4002135 | *Bioconjugate Chem.* 2013, 24, 1684−1697

The accumulation of the GPI-APs in lipid rafts may serve as platforms for diverse cellular functions (e.g., signal transduction) by promoting protein−protein interactions.[23,24] Beyond the membrane anchoring, other biological functions of the GPIs associated with the carbohydrate moiety are rather unknown, partly because the complexity of the GPIs restricts the preparation of GPI-AP derivatives for structural and functional studies. However, a few studies have been published on the semisynthesis of proteins with simplified anchors, and on their subsequent delivery to membrane structures,[25−34] and it was shown that the removal of the carbohydrate moiety or its truncation does not interfere with the anchoring function of the GPI.[35]

An important feature of the GPI-APs is that they spontaneously reintegrate into model lipid membranes, or live cell membranes with the retention of the biological function.[36−44] This property of the GPI-APs may be exploited for structural and functional studies, because semisynthetic lipoproteins containing GPI anchor mimetic lipids can also be introduced into cell membranes by exogenous addition. Since cholesterol prefers the interaction with sphingolipids in the cell membrane, it has the potential to target the attached protein to lipid rafts.[20,21] This type of lipid anchor is found in the matured Hh and Shh proteins of the hedgehog family as a C-terminal cholesteryl ester.[45−48] Furthermore, in the case of a semisynthetic peptidyl cholesterol−Ras protein conjugate, cholesterol was reported to anchor the conjugated protein to the cell membrane.[49] Other cholesterol derivatives, such as 3β-cholesterylamine and 3β-cholesterylcarbamate, were also reported as membrane anchors of artificial membrane receptors.[50−56]

Here, we report on the development of a fluorescent cholesterol anchor as a GPI mimetic, and on its insertion into the plasma membrane of live cells. Fluorescent labeling is generally required when the cellular traffic of a membrane protein is to be monitored, and that is usually achieved by fusion of a fluorescent reporter protein to the target protein. However, the size of the reporter protein is frequently comparable to that of the target protein, and it can perturb the biophysical and biochemical characteristics of the target protein. In order to avoid this drawback, our approach utilizes a small molecule fluorophore for facilitating the imaging of membrane anchored proteins. The fluorescent reporter is introduced into the headgroup of the membrane anchor; therefore, its interference with the lipid chains in the cell membrane is unlikely. Furthermore, it might have minimal effect on protein−protein interactions between the membrane anchored protein and other cell surface proteins. This anchor was used for the semisynthesis of a cholesteryl lipoprotein to demonstrate the usefulness of this protein lipidation approach. Before imaging applications, the separation of the semisynthetic fluorescent lipoprotein from the micellar associates of the amphiphilic fluorescent lipids without denaturing the native fold of the protein is a crucial step. When it is achieved, the fluorescence of the cholesterol anchor can be unambiguously assigned to the attached protein, and thus, the protein can be visualized after cell membrane delivery of the semisynthetic construct. On the whole, our method can be utilized for imaging the cellular traffic of lipoproteins and also for investigating protein−protein interactions on the cell surface.

EXPERIMENTAL SECTION

Synthesis of the Cholesterol Probe. *Cholesteryl 1-(Triphenylmethylamino)-15-oxo-4,7,10-trioxa-14-azaoctadecan-18-oate (**1**).* Cholesteryl hemisuccinate (150 mg, 0.31 mmol) and TBTU (100 mg, 0.31 mmol) were dissolved in 10 mL of $CHCl_3/CH_2Cl_2$ (4:1), and DIEA (68 μL, 0.40 mmol) was added. After 5 min activation 1-(triphenylmethylamino)-13-amino-4,7,10-trioxa-tridecane (143 mg, 0.31 mmol) was added to the solution. The mixture was stirred for 8 h at RT, then it was evaporated in vacuo. The crude product was purified by column chromatography ($CHCl_3$/MeOH (99:1)) to give 274.6 mg (95%) of **1** as a white solid. R_f 0.5 ($CHCl_3$/MeOH = 99:1); k′ = 4.63 (t_R = 20.05 min; Alltech Alltima HP C18 column (250 × 4.6 mm, 5 μm), isocratic elution with ACN/MeOH 15:85, flow rate: 1 mL/min, λ = 215 nm); $[\alpha]_D^{20}$ = −10.0 (c = 1.1, $CHCl_3$); ^{1}H NMR (500 MHz, $CDCl_3$) δ 7.47 (d, 6H, J = 7.5 Hz, Trt-o-H), 7.26 (t, 6H, J = 7.5 Hz, Trt-m-H), 7.17 (t, 3H, J = 7.2 Hz, Trt-p-H), 6.31 (t, 1H, J = 5.0 Hz, amide NH), 5.36 (d, 1H, J = 3.0 Hz, 6-H), 4.60 (m, 1H, 3α-H), 3.57 (m, 12H, 34-H, 35-H, 36-H, 37-H, 38-H, 39-H), 3.35 (q, 2H, J = 5.8 Hz, 32-H), [2.61 (t, 2H, J = 6.9 Hz), 2.42 (t, 2H, J = 6.9 Hz)] (29-H, 30-H), 2.31 (d, 2H, J = 7.8 Hz, 4-H), 2.22 (t, 2H, J = 5.5 Hz, 41-H), 2.01 (m, 1H, 12β-H), 1.98 (m, 1H, 7β-H), 1.84 (m, 3H, (1β-H, 2α-H, 16α-H)), 1.76 (m, 4H, 33-H, 40-H), [1.64−1.04 (m, 18H): 2β-H, 12α-H, 15α/β-H, 1.55 (7α-H), 1.52 (25-H), 1.46 (11α/β-H), 1.42 (8β-H), 1.35 (23-H), 1.33 (20-H, 22-H), 1.23 (16β-H), 1.18 (23-H′), (1.14, 1.09) (1α-H, 17α-H), 1.12 (24-H_2)], [1.04−0.90 (m, 3H): 0.96 (14α-H, 22-H′), 0.92 (9α-H)], 1.01 (s, 3H, 19-H), 0.92 (d, 3H, J = 6.3 Hz, 21-H), [0.88 (d, 3H, J = 1.5 Hz), 0.86 (d, 3H, J = 1.5 Hz)] (26-H, 27-H), 0.68 (s, 3H, 18-H); ^{13}C NMR (125 MHz, $CDCl_3$) δ 172.5 (ester CO), 171.4 (amide CO), 146.4 (Ph C_q), 139.7 (C-5), 128.8 (Ph o-CH), 127.9 (Ph m-CH), 126.3 (Ph p-CH), 122.7 (C-6), 74.3 (C-3), 71.0 ($\underline{C}Ph_3$), [70.7 (2C), 70.4, 70.2 (3C)] (C-34, C-35, C-36, C-37, C-38, C-39), (56.8, 56.3) (C-14, C-17), 50.2 (C-9), 42.4 (C-13), 41.1 (C-41), 39.9 (C-12), 39.6 (C-24), 38.2 (2C, C-4, C-32), 37.1 (C-1), 36.7 (C-10), 36.3 (C-22), 35.9 (C-20), 32.1 (C-7), 32.0 (C-8), (31.2, 30.1) (C-29, C-30), 30.7 (C-40), 29.0 (C-16), 28.4 (C-33), 28.1 (C-25), 27.9 (C-2), 24.4 (C-15), 24.0 (C-23), (22.9, 22.7) (C-26, C-27), 21.2 (C-11), 19.4 (C-19), 18.9 (C-21), 12.0 (C-18); MS(MALDI) calcd for $C_{60}H_{86}N_2O_6$ 930.65, found 931.67 $[M+H]^+$, 689.52 $[(M-Trt)+2H]^+$; ATR FT-IR 3310, 3082, 3055, 3028, 2933, 2866, 1728, 1641, 1547, 1489, 1447, 1171, 1107, 1029, 1001, 772, 745, 706, 644, 623 cm^{-1}.

*Cholesteryl 1-Amino-15-oxo-4,7,10-trioxa-14-azaoctadecan-18-oate (**2**).* The tritylamine **1** (145 mg, 0.16 mmol) was dissolved in 5 mL of CH_2Cl_2 containing 10% (v/v) TFA and 5% (v/v) triisopropylsilane, and it was stirred for 10 min. The solution was evaporated in vacuo and the cleavage was repeated four times. The product was purified by column chromatography (AcOH/MeOH (2:98)) to give 120.7 mg (94%) of pure **2** as a pale yellow solid. R_f 0.52 (AcOH/MeOH = 2:98); k′ = 3.71 (t_R = 16.77 min, Alltech Alltima HP C18 column (250 × 4.6 mm, 5 μm), isocratic elution with ACN/MeOH 15:85, flow rate: 1 mL/min, λ = 215 nm); MS(MALDI) calcd for $C_{41}H_{72}N_2O_6$ 688.54, found 689.54 $[M+H]^+$.

*Cholesterol Probe (**3**).* The amine **2** (91 mg, 0.11 mmol) was dissolved in 5 mL of DMF and then DIEA (19 μL, 0.11 mmol) was added. The solution of fluorescein-5-isothiocyanate (51 mg, 0.13 mmol) and DIEA (57 μL, 0.33 mmol) in 1.5 mL

dx.doi.org/10.1021/bc4002135 | Bioconjugate Chem. 2013, 24, 1684−1697

DMF was added in three portions over 6 h at RT. Then, it was evaporated in vacuo and the crude product was purified by column chromatography ($CHCl_3$/acetone/AcOH 60:39:1) followed by ($CHCl_3$/MeOH/AcOH 94:5:1) to give 55.6 mg (47%) of pure **3** as an orange solid. R_f 0.54 ($CHCl_3$/acetone/AcOH = 60:39:1), 0.36 ($CHCl_3$/MeOH/AcOH = 94:5:1); k′ = 1.25 (t_R = 7.95 min; Alltech Alltima HP C18 column (250 × 4.6 mm, 5 μm), isocratic elution with ACN/MeOH 15:85, flow rate: 1 mL/min, λ = 215 nm); $[\alpha]_D^{20}$ = −9.4 (*c* = 0.32, $CHCl_3$); ^{1}H NMR (500 MHz, $(CD_3)_2SO$) δ 10.17 (brs, Ar−OH), 9.95 (brs, 1H, CS-NH-Ar), 8.23 (s, 1H, 4′-H), 8.10 (brs, 1H, CS-NH-CH_2), 7.79 (t, 1H, *J* = 5.3 Hz, CO-NH), 7.73 (d, 1H, *J* = 5.3 Hz, 6′-H), 7.14 (d, 1H, *J* = 8.2 Hz, 7′-H), 6.65 (d, 2H, *J* = 1.4 Hz, 4″-H), 6.59 (d, 2H, *J* = 8.6 Hz, 1″-H), 6.54 (dd, 2H, *J* = 8.7 Hz, 1.6 Hz, 2″-H), 5.30 (s, 1H, 6-H), 4.42 (m, 1H, 3-H), 3.50 (m, 10H, 35-H, 36-H, 37-H, 38-H, 41-H), 3.36 (m, 4H, 34-H, 39-H), 3.06 (q, 2H, *J* = 6.4 Hz, 32-H), 2.44 (t, 2H, *J* = 6.7 Hz, 30-H), 2.30 (t, 2H, *J* = 6.7 Hz, 29-H), 2.22 (d, 2H, *J* = 7.5 Hz, 4-H), 1.90 (m, 2H, 7β-H, 12β-H), 1.80 (quin, 2H, *J* = 6.5 Hz, 40-H), 1.75 (m, 3H, 1β-H, 2α-H, 16α-H), 1.59 (quin, 2H, *J* = 6.5 Hz, 33-H), [1.55−0.89 (m, 21H): 1.50 (2β-H, 15α-H), 1.48 (7α-H), 1.46 (25-H), 1.45 (11-α/β-H), 1.36 (8β-H), 1.30 (22-H, 23-H), 1.29 (20-H), 1.20 (16β-H), 1.10 (23-H′), 1.09 (12α-H, 15β-H, 24-H_2), (1.05, 0.95) (14α-H, 17α-H), 1.01 (1α-H), 0.95 (22-H′), 0.89 (9α-H)], 0.94 (s, 3H, 19-H), 0.86 (d, 3H, *J* = 6.2 Hz, 21-H), [0.82 (d, 3H, *J* = 1.6 Hz), 0.81 (d, 3H, *J* = 1.6 Hz)] (26-H, 27-H), 0.62 (s, 3H, 18-H); ^{13}C NMR (125 MHz, $(CD_3)_2SO$) δ 180.5 (CS), 171.7 (ester CO), 170.6 (amide CO), 168.5 (lactone CO), (159.7, 152.0) (C-3″, C-4″a), (146.8, 141.4) (C-5′, C-8′), 139.5 (C-5), 129.2 (C-6′), 129.0 (C-1″), 126.7 (C-3′), 124.0 (C-7′), 122.1 (C-6), 116.4 (C-4′), 112.7 (C-2″), 109.9 (C-1″a), 102.3 (C-4″), 83.5 (C-9″), 73.2 (C-3), [69.8 (2C), 69.6 (2C)] (C-35, C-36, C-37, C-38), (68.2, 68.1) (C-34, C-39), (56.2, 55.7) (C-14, C-17), 49.5 (C-9), 41.9 (C-13), 41.4 (C-41), 39.2 (C-12), 39.0 (C-24), 37.7 (C-4), 36.5 (C-1), 36.1 (C-10), 35.9 (C-32), 35.7 (C-22), 35.3 (C-20), 31.4 (C-8), 31.3 (C-7), 30.0 (C-29), 29.4 (2C, C-30, C-33), 28.6 (C-40), 27.8 (C-16), 27.4 (C-25), 27.3 (C-2), 23.9 (C-15), 23.3 (C-23), (22.7, 22.4) (C-26, C-27), 20.6 (C-11), 19.0 (C-19), 18.6 (C-21), 11.7 (C-18); MS(MALDI) calcd for $C_{62}H_{83}N_3O_{11}S$ 1077.57, found 1078.58 $[M+H]^+$; ATR FT-IR 3600−2400 br, 3300, 3092, 2934, 2866, 1730, 1611, 1587, 1539, 1504, 1464, 1447, 1375, 1331, 1254, 1213, 1171, 1109, 1078, 1024, 993, 849, 824, 787, 671 cm^{-1}.

Investigation of the *in Vitro* Hydrolytic Stability of the Cholesteryl Ester in Probe 3. The cholesterol probe **3** (150 μM) was dissolved in PBS buffer containing 5% (v/v) HFIP. Samples were taken over a period of 24 h and were analyzed by RP-HPLC on an Alltech Alltima HP C18 column (250 × 4.6 mm, 5 μm) with isocratic elution (ACN/MeOH 15:85) at a flow rate of 1 mL/min, λ = 216 nm. The probe **3** peak area values of the samples were compared to that of the starting solution.

Synthesis of the Cholesterol Anchor. *(S)-N-(2-Maleimidoethyl)-2-(tert-butoxycarbonylamino)pent-4-ynamide (**4**).* *N*-(2-(*tert*-butoxycarbonylamino)-ethyl)-maleimide (100 mg, 0.41 mmol) was dissolved in 10 mL of TFA/CH_2Cl_2 1:1 and the solution was stirred for 30 min, then it was evaporated in vacuo. The resulting *N*-(2-aminoethyl)maleimide trifluoroacetate was used without further purification. Boc-Pra-OH (81.3 mg, 0.38 mmol) and HOBt (58.2 mg, 0.38 mmol) were dissolved in THF (6 mL) and DIC (58.8 μL, 0.38 mmol) was added. After 5 min stirring *N*-(2-aminoethyl)maleimide trifluoroacetate (96.6 mg, 0.38 mmol) and DIEA (65 μL, 0.38 mmol) in THF (1 mL) were added, and the reaction mixture was stirred for 8 h at RT. It was diluted with 20 mL of EtOAc and then extracted with 0.5 M HCl (3 × 20 mL). The combined organic layer was dried over Na_2SO_4 and evaporated in vacuo. The crude product was purified by column chromatography ($CHCl_3$/acetone 4:1) to give 114.5 mg (90%) of pure **4** as a white solid. R_f 0.4 ($CHCl_3$/acetone 4:1); k′ = 3.86 (t_R = 17.0 min; Alltech Alltima HP C18 column (250 × 4.6 mm, 5 μm), linear gradient of 5→95% B in A over 30 min (eluent A: 0.1% (v/v) TFA in H_2O, eluent B: 0.08% (v/v) TFA in ACN), flow rate: 1 mL/min, λ = 216 nm); $[\alpha]_D^{20}$ = −2.6 (*c* = 1, $CHCl_3$); ^{1}H NMR (500 MHz, $(CD_3)_2SO$) δ 8.06 (t, 1H, *J* = 5.2 Hz, amide NH), 6.98 (s, 2H, maleimide CH), 6.81 (d, 1H, *J* = 8.5 Hz, carbamate NH), 3.95 (dt, 1H, *J* = 8.5, 4.5 Hz, α-H), 3.43 (t, 2H, *J* = 5.7 Hz, 1-H), 3.30 (m, 1H, 2-H), 3.10 (m, 1H, 2-H′), 2.77 (s, 1H, δ-H), 2.44 (ddd, 1H, *J* = 16.7, 4.5, 2.5 Hz, β-H), 2.32 (ddd, 1H, *J* = 16.7, 9.1, 1.6 Hz, β-H′), 1.36 (s, 9H, Boc-CH_3); ^{13}C NMR (125 MHz, $(CD_3)_2SO$) δ 171.0 (maleimide CO), 170.5 (Pra CO), 155.1 (carbamate CO), 134.5 (maleimide CH), 81.0 (C-γ), 78.2 (C(CH_3)$_3$), 72.6 (C-δ), 53.2 (C-α), [37.0, 36.9] (C-1, C-2), 28.2 (CH_3), 21.8 (C-β); MS(ESI) calcd for $C_{16}H_{21}N_3O_5$ 335.15, found 335.90 $[M+H]^+$, FT-IR (KBr) 3341, 3323, 3273, 3098, 2968, 2926, 2874, 2855, 2116, 1703, 1688, 1661, 1616, 1574, 1560, 1531, 1464, 1418, 1387, 1362, 1325, 1273, 1252, 1171, 1130, 1105, 1053, 961, 866, 826, 804, 686 (br) cm^{-1}.

*(S)-N-(2-Maleimidoethyl)-2-aminopent-4-ynamide (**5**).* N^{α}-*t*-Butyloxycarbonyl-propargyl-glycine-*N*-(2-maleimidoethyl)-amide (**4**) (20.0 mg, 60 μmol) was dissolved in 2 mL of TFA/CH_2Cl_2 1:1 and it was stirred for 30 min. The solution was evaporated in vacuo to give 20.1 mg (96%) of pure **5** as a pale yellow solid. R_f 0.4 ($CHCl_3$/MeOH 95:5); HPLC: k′ = 1.23 (t_R = 7.8 min; Alltech Alltima HP C18 column (250 × 4.6 mm, 5 μm), linear gradient of 5→95% B in A over 30 min (eluent A: 0.1% (v/v) TFA in H_2O, eluent B: 0.08% (v/v) TFA in ACN), flow rate: 1 mL/min, λ = 216 nm); MS(ESI) calcd for $C_{11}H_{13}N_3O_3$ 235.10, found 236.20 $[M+H]^+$.

*(S)-2-(3-(5-Fluoresceinyl-thioureido)-N-(2-maleimidoethyl)pent-4-ynamide (**6**).* Propargyl-glycine-*N*-(2-maleimidoethyl)amide (**5**) (20.1 mg, 57.6 μmol) was dissolved in THF (0.5 mL) and then fluorescein-5-isothiocyanate (23.4 mg, 60 μmol) and DIEA (10.3 μL, 60 μmol) were added to the solution; then, it was stirred for 13 h. After evaporation in vacuo the crude product was purified by HPLC (Vydac 218TP1010 column (250 × 10 mm, 10 μm), linear gradient of 5→95% B in A over 30 min (eluent A: 0.1% (v/v) TFA in H_2O, eluent B: 0.08% (v/v) TFA in ACN), flow rate: 4 mL/min, λ = 216 nm) to give 25.8 mg (69%) of pure **6** as an orange solid. R_f 0.4 ($CHCl_3$/MeOH 95:5); HPLC: k′ = 4.31 (t_R = 18.6 min; Alltech Alltima HP C18 column (250 × 4.6 mm, 5 μm), linear gradient of 5→95% B in A over 30 min (eluent A: 0.1% (v/v) TFA in H_2O, eluent B: 0.08% (v/v) TFA in ACN), flow rate: 1 mL/min, λ = 216 nm); $[\alpha]_D^{20}$ = −3.9 (*c* = 0.7, MeOH); ^{1}H NMR (500 MHz, $(CD_3)_2SO$) δ 10.41 (brs, 1H, CS-NH-Ar), 10.10 (brs, Ar-OH), 8.44 (s, 1H, 4′-H), 8.37 (t, 1H, *J* = 5.8 Hz, CONH), 8.14 (d, 1H, *J* = 7.4 Hz, CS-NH-Cα), 7.77 (dd, 1H, *J* = 8.3, 1.6 Hz, 6′-H), 7.18 (d, 1H, *J* = 8.3 Hz, 7′-H), 7.00 (s, 2H, maleimide CH), 6.66 (d, 2H, *J* = 1.9 Hz, 4″-H), 6.59 (d, 2H, *J* = 8.2 Hz, 1″-H), 6.55 (dd, 2H, *J* = 8.7, 2.0 Hz, 2″-H), 4.88 (q, 1H, *J* = 5.6 Hz, α-H), 3.48 (m, 2H, 1-H), 3.33 (m, 1H, 2-H), 3.27 (m, 1H, 2-H′), 2.85 (t, 1H, *J* = 2.4 Hz, δ-H), 2.80 (ddd, 1H, *J* = 17.0, 5.2, 2.4 Hz, β-H), 2.62 (ddd, 1H, *J* = 17.0,

dx.doi.org/10.1021/bc4002135 | *Bioconjugate Chem.* 2013, 24, 1684−1697

5.1, 2.3 Hz, β-H′); ^{13}C NMR (125 MHz, $(CD_3)_2SO$) δ 179.8 (CS), 171.1 (maleimide CO), 169.5 (CONH), 168.6 (lactone CO), (159.5, 151.9) (C-3″, C-4″a), (147.3, 141.3) (C-5′, C-8′), 134.6 (maleimide CH), 129.2 (C-6′), 129.1 (C-1″), 126.5 (C-5′), 124.1 (C-7′), 116.2 (C-4′), 112.6 (C-2″), 109.7 (C-1″a), 102.3 (C-4″), 79.9 (C-δ), 73.7 (C-γ), 55.3 (C-α), 37.0 (2C, C-1, C-2), 22.1 (C-β); MS(ESI) calcd for $C_{32}H_{24}N_4O_8S$ 624.13, found 625.00 $[M+H]^+$; FT-IR (KBr) 3433 br, 3267 (br), 3065, 2995, 2884, 2822, 2683, 2560, 1744, 1680, 1639, 1612, 1589, 1578, 1510, 1460, 1425, 1317, 1287, 1206, 1182, 1136, 1113, 783, 739 cm^{-1}.

*Cholesteryl 1-Azido-13-oxo-3,6,9-trioxa-12-azahexadecan-16-oate (**7**).* Cholesteryl hemisuccinate (200 mg, 0.41 mmol) and TBTU (171 mg, 0.53 mmol) were dissolved in 6 mL of $CHCl_3/CH_2Cl_2$ (4:1), and DIEA (91.3 μL, 0.53 mmol) was added. It was stirred for 5 min, then 1-amino-11-azido-3,6,9-trioxaundecane (89.5 mg, 0.41 mmol) was added to the solution. The mixture was stirred for 8 h at RT, then it was evaporated in vacuo. The crude product was purified by column chromatography with $CHCl_3$/MeOH (97:3) to give 253.5 mg (90%) of **7** as a white solid. R_f 0.40 ($CHCl_3$/MeOH = 97:3); k′(HPLC) = 2.33 (t_R = 14.5 min; Alltech Alltima HP C18 column (250 × 4.6 mm, 5 μm), isocratic elution with ACN/MeOH (15:85), flow rate: 1 mL/min, λ = 216 nm); $[\alpha]_D^{20}$ = −26.0 (*c* = 1.7, $CHCl_3$); ^{1}H NMR (500 MHz, $CDCl_3$) δ 6.20 (brs, 1H, NH), 5.36 (d, 1H, *J* = 3.3 Hz, 6-H), 4.61 (m, 1H, 3α-H), 3.68 (m, 8H, 34-H, 35-H, 36-H, 37-H), 3.63 (m, 2H, 38-H), 3.55 (t, 2H, *J* = 4.9 Hz, 33-H), 3.45 (q, 2H, *J* = 4.6 Hz, 32-H), 3.40 (t, 2H, *J* = 4.7 Hz, 39-H), [2.64 (t, 2H, *J* = 6.8 Hz), 2.48 (t, 2H, *J* = 6.8 Hz)] (29-H, 30-H), 2.31 (d, 2H, *J* = 7.7 Hz, 4-H), 2.03 (m, 1H, 12β-H), 1.96 (m, 1H, 7β-H), 1.89 (m, 1H, 2α-H), 1.87 (m, 1H, 1β-H), 1.83 (m, 1H, 16α-H), [1.62−1.04 (m, 18H): 1.56 (2β-H, 15α-H), 1.53 (7α-H), 1.52 (25-H), 1.47 (11α/β-H), 1.44 (8β-H), 1.36 (23-H), 1.34 (20-H, 22-H), 1.20 (16β-H), 1.17 (23-H′), 1.15 (12α-H), 1.12 (1α-H), 1.11 (24-H_2), 1.09 (17α-H), 1.06 (15β-H)], 1.01 (s, 3H, 19-H), [1.03−0.90 (m, 3H): 0.99 (14α-H, 22-H′), 0.94 (9α-H)], 0.91 (d, 3H, *J* = 6.7 Hz, 21-H), [0.86 (d, 3H, *J* = 1.9 Hz), 0.85 (d, 3H, *J* = 1.9 Hz)] (26-H, 27-H), 0.67 (s, 3H, 18-H); ^{13}C NMR (125 MHz, $CDCl_3$) δ 172.2 (ester CO), 171.4 (amide CO), 139.6 (C-5), 122.6 (C-6), 74.3 (C-3), [70.7, 70.6, 70.5, 70.3, 70.0, 69.8] (C-33, C-34, C-35, C-36, C-37, C-38), 56.7 (C-14), 56.1 (C-17), 50.7 (C-39), 50.0 (C-9), 42.3 (C-13), 39.7 (C-12), 39.5 (C-24), 39.3 (C-32), 38.1 (C-4), 37.0 (C-1), 36.6 (C-10), 36.2 (C-22), 35.8 (C-20), 31.9 (C-7), 31.8 (C-8), [31.0, 29.9] (C-29, C-30), 28.2 (C-16), 28.0 (C-25), 27.7 (C-2), 24.3 (C-15), 23.8 (C-23), [22.8, 22.6] (C-26, C-27), 21.0 (C-11), 19.3 (C-19), 18.7 (C-21), 11.8 (C-18); MS(MALDI) calcd for $C_{39}H_{66}N_4O_6$ 686.50, found 687.62 $[M+H]^+$, 659.57 $[(M-N_2)+H]^+$; ATR FT-IR 3314, 2951, 2930, 2866, 2104, 1730, 1647, 1547, 1466, 1441, 1375, 1366, 1327, 1304, 1283, 1254, 1171, 1124, 1028, 999, 627, 530 cm^{-1}.

*Cholesterol Anchor (**8**).* The alkyne **6** (42 mg, 67.2 μmol) and the azide **7** (46 mg, 67.2 μmol) were dissolved in *t*BuOH (0.9 mL). The solution of L(+)-ascorbic acid sodium salt (7.9 mg, 39.9 μmol) and $CuSO_4 \cdot 5H_2O$ (5.0 mg, 20.1 μmol) in 0.9 mL of water were added and the reaction mixture was stirred for 48 h at RT. Then it was evaporated in vacuo and the crude product was purified by column chromatography ($CHCl_3$/MeOH/AcOH 90:9:1) to give 58 mg (66%) of pure **8** as an orange solid. R_f 0.4 ($CHCl_3$/MeOH/AcOH 90:9:1); k′ = 5.20 (t_R = 12.4 min; Vydac 214TP5410 C4 column (100 × 4.6 mm, 5 μm), linear gradient of 50→95% B in A over 25 min (eluent A: 0.1% (v/v) TFA in H_2O, eluent B: 0.08% (v/v) TFA in ACN), flow rate: 1 mL/min, λ = 216 nm); $[\alpha]_D^{20}$ = −32.9 (*c* = 0.65, $CHCl_3$); ^{1}H NMR (500 MHz, $(CD_3)_2SO$) δ 10.31 (s, 1H, CS-NH-Ar), 10.19 (brs, Ar-OH), 8.39 (s, 1H, 4″-H), 8.32 (t, 1H, *J* = 5.6 Hz, α-CONH), 8.10 (d, 1H, *J* = 5.3 Hz, CS-NH-Cα), 7.87 (t, 1H, *J* = 5.3 Hz, 32-NH), 7.79 (s, 1H, triazole CH), 7.74 (d, 1H, *J* = 8.2 Hz, 6″-H), 7.15 (d, 1H, *J* = 8.2 Hz, 7″-H), 7.00 (s, 2H, maleimide CH), 6.64 (s, 2H, 4‴-H), 6.59 (dd, 2H, *J* = 8.6, 2.6 Hz, 1‴-H), 6.53 (dd, 2H, *J* = 8.6, 1.6 Hz, 2‴-H), 5.30 (d, 1H, *J* = 3.2 Hz, 6-H), 5.04 (q, 1H, *J* = 5.9 Hz, α-H), 4.47 (t, 2H, *J* = 5.0 Hz, 39-H), 4.41 (m, 1H, 3-H), 3.76 (t, 2H, *J* = 5.0 Hz, 38-H), 3.47 (m, 2H, 1′-H), 3.44 (brs, 8H, 34-H, 35-H, 36-H, 37-H), 3.35 (t, 2H, *J* = 5.9 Hz, 33-H), 3.28 (m, 1H, 2′-H), 3.22 (dd, 1H, *J* = 14.0, 6.3 Hz, 2′-H′), 3.16 (q, 2H, *J* = 5.7 Hz, 32-H), 3.15 (m, 1H, β-H), 3.03 (dd, 1H, *J* = 14.9, 7.1 Hz, β-H′), [2.43 (t, 2H, *J* = 6.6 Hz), 2.31 (t, 2H, *J* = 6.7 Hz)] (29-H, 30-H), 2.22 (d, 2H, *J* = 7.6 Hz, 4-H), 1.93 (m, 1H, 12β-H), 1.87 (m, 1H, 7β-H), 1.75 (m, 3H, 1β-H, 2α-H, 16α-H), [1.56−0.89 (m, 21H): 1.50 (2β-H, 15α-H), 1.47 (7α-H), 1.46 (25-H), 1.45 (11-α/β-H), 1.36 (8β-H), 1.30 (20-H, 22-H, 23-H), 1.19 (16β-H), 1.12 (23-H′), 1.09 (12α-H, 15β-H, 24-H_2), 1.05 (17α-H), 0.96 (14α-H), 1.00 (1α-H), 0.97 (22-H′), 0.88 (9α-H)], 0.94 (s, 3H, 19-H), 0.87 (d, 3H, *J* = 6.4 Hz, 21-H), [0.83 (d, 3H, *J* = 2.0 Hz), 0.82 (d, 3H, *J* = 2.0 Hz)] (26-H, 27-H), 0.62 (s, 3H, 18-H); ^{13}C NMR (125 MHz, $(CD_3)_2SO$) δ 180.0 (CS), 171.7 (ester CO), 171.1 (maleimide CO), 170.8 (30-CO), 170.4 (α-CO), 168.6 (lactone CO), (159.8, 152.1) (C-3‴, C-4‴a), (147.2, 141.2) (C-5″, C-8″), 142.2 (triazole C_q), 139.6 (C-5), 134.6 (maleimide CH), 129.3 (C-6″), 129.1 (C-1‴), 126.8 (C-3″), 124.2 (C-7″), 123.3 (triazole CH), 122.1 (C-6), 116.4 (C-4″), 112.7 (C-2‴), 109.8 (C-1‴a), 102.3 (C-4‴), 83.3 (C-9‴), 73.2 (C-3), [69.72, 69.69, 69.64, 69.58, 69.1, 68.9] (C-33, C-34, C-35, C-36, C-37, C-38), 56.7 (C-α), 56.1 (C-14), 55.6 (C-17), 49.5 (C-9), 49.3 (C-39), 41.9 (C-13), 39.0 (2C, C-12, C-24), 38.6 (C-32), 37.7 (C-4), 37.0 (2C, C-1′, C-2′), 36.5 (C-1), 36.1 (C-10), 35.7 (C-22), 35.2 (C-20), 31.4 (C-8), 31.3 (C-7), [29.9, 29.3] (C-29, C-30), 28.3 (C-β), 27.8 (C-16), 27.4 (C-25), 27.3 (C-2), 23.9 (C-15), 23.2 (C-23), [22.7, 22.4] (C-26, C-27), 20.6 (C-11), 19.0 (C-19), 18.6 (C-21), 11.7 (C-18); MS(MALDI) calcd for $C_{71}H_{90}N_8O_{14}S$ 1310.63, found 1311.63 $[M+H]^+$; ATR FT-IR 3600−2400 br, 3275, 3066, 2936, 2904, 2868, 1709, 1659, 1639, 1587, 1502, 1464, 1406, 1381, 1329, 1254, 1207, 1175, 1107, 1028, 993, 914, 850, 826, 696, 671 cm^{-1}.

Expression and Purification of mCherry Extended with a C-terminal Cys (mCherry-Cys). Cys extended mCherry with a His_6 tag (Figure S6) was cloned into a modified pRSET vector (Invitrogen). Transformed cells of *E. coli* BL21(DE3) were grown at 37 °C in 1 L of LB medium containing 100 μg/mL ampicillin. When OD_{600} = 0.6 was achieved, the protein expression was induced by isopropyl-1-thio-β-D-galactopyranoside in a final concentration of 0.5 mM. Cells were grown for further 4 h at 37 °C, and then harvested by centrifugation at 5000 rpm for 15 min at 4 °C. The pellet was resuspended in 40 mL of 50 mM Na_2HPO_4, 300 mM NaCl, 10 mM imidazole, pH 8.0 containing a protease inhibitor cocktail of Sigma, and cells were disrupted by sonication at 4 °C. The lysate was centrifuged at 15000 rpm for 30 min and the supernatant was applied to a Ni-NTA column equilibrated with the same buffer. The column was washed with 5 column volumes of 50 mM Na_2HPO_4, 300 mM NaCl, 20 mM imidazole, pH 8.0, and then the mCherry was eluted with 50 mM Na_2HPO_4, 300 mM NaCl, 250 mM imidazole, pH 8.0.

dx.doi.org/10.1021/bc4002135 | *Bioconjugate Chem.* 2013, 24, 1684−1697

Fractions containing the target protein were desalted on Sephadex G-25 columns with Milli-Q water and stored at −20 °C as a frozen solution.

Conjugation of the Cholesterol Anchor to mCherry-Cys. The protein conjugation of the cholesterol anchor was investigated by the addition of different molar excess of **8** to the solution of mCherry (1 mg/mL, 36 μM) in 20 mM Tris, 10 mM TCEP, pH 7.5, and it was incubated at 20 °C for 1 h. Then, 100 μL of the reaction mixture was introduced to a Superdex 75 column and eluted with 50 mM Na_2HPO_4, 150 mM NaCl, pH 7.0 (Figure S4). On preparative scale, a protein:anchor ratio of 1:10 was applied, and the total amount of **8** was added in 10 portions over 5 h. The mixed micelles composed of the cholesteryl lipoprotein and the cholesterol anchor was purified by size-exclusion chromatography on Superdex 75, and then the mixed micellar associates were incubated with 10 equiv β-cyclodextrin at 20 °C for 24 h. The inclusion complex of **8** and that of the protein−anchor conjugate was separated with size-exclusion chromatography.

ECD Spectroscopy. ECD spectra of mCherry-Cys and the mCherry−anchor conjugate in the 190−250 nm region were recorded on a Jasco (Tokyo, Japan) J815 spectropolarimeter, equipped with a Peltier temperature controller, at 25 °C and 100 nm/s scan speed using a 1 mm path length quartz cell. Protein concentration of the samples was in the 2.5−6.5 μM range as measured by the Bradford method.[57] Spectra presented here are accumulations of 10 scans and the corresponding solvent spectra recorded under the same conditions were subtracted. The contribution of each secondary structural element of the protein was determined by deconvolution of the spectra using the CDSSTR method.[58]

Cell Culture. For *in vitro* biological studies, SH-SY5Y (ATCC: CRL-2266) human neuroblastoma cells were used. They were cultured in DMEM (Sigma Ltd., St. Louis, MO, USA) medium containing 10% FCS, L-glutamine (2 mM), gentamycin (160 μg/mL), 1 mM pyruvate, and nonessential amino acids (Sigma Ltd., St. Louis, MO, USA). The cultures of cells were maintained at 37 °C in a humidified atmosphere with 5% CO_2.

***In Vitro* Cytotoxic Effect of the Cholesterol Anchor and the mCherry−Anchor Conjugate.** The *in vitro* cytotoxic effect of **8** and the mCherry−anchor **8** conjugate was evaluated by the MTT-assay.[59] For the experiment, 5×10^3 cells per well were plated on 96-well plates. After 24 h incubation at 37 °C, cells were treated with **8** or with mCherry−anchor **8** dissolved in serum-free medium (0.26 nM − 100 μM and 0.26 nM − 10 μM, respectively) for 60 min. The control cells were treated with serum-free medium for 60 min. MTT solution was added to the cells at a final concentration of 367 μg/mL; after 3.5 h incubation they were centrifuged for 5 min at 863 × *g* and the supernatant was removed. The formazan crystals were dissolved in DMSO and the absorbance (A) of the samples was measured at λ = 540 and 620 nm using an ELISA Reader (Labsystems MS reader, Finland). A_{620} was subtracted from A_{540} and the percent of cytotoxicity was calculated using the following equation:

$$\text{Cytotoxicity (\%)} = [1 - (A_{\text{treated}}/A_{\text{control}})] \times 100$$

where A_{treated} and A_{control} correspond to the absorbance of the treated and control cells, respectively.

Live Cell Imaging with Confocal Laser Scanning Microscopy. 20 000 cells per well were plated on an 8-well Lab-Tek II Chambered coverglass. After 48 h incubation at 37 °C, cells were treated with **3**, **8**, or mCherry−anchor **8** dissolved in serum-free medium for 30 min. The concentration of the cholesterol probe and the cholesterol anchor was 1 μM, while the mCherry−anchor **8** conjugate was applied at 10 μM concentration. Cells treated with serum-free medium for 30 min were used as a negative control. After treatment and incubation, cells were washed with serum-free medium and the nuclei of the cells were stained for 5 min using the nuclear dye DRAQ5. Sequential excitation was applied for fluorescein, mCherry, and DRAQ5. Fluorescein was excited with an Ar ion laser (488 nm) and emitted photons were collected through a BA 505−525 nm filter; mCherry was excited with a He−Ne laser at 543 nm and emitted photons were collected through a BA 595−615 nm filter; DRAQ5 was excited with a He−Ne laser at 633 nm and emitted photons were collected through a BA 660 nm filter. The colocalization of mCherry and fluorescein signals was quantitated on 15 confocal microscopy images with more than 600 cells. In our case the intensities of the two fluorescent signals were different (Figure 7, emission spectra); therefore, Manders colocalization coefficients were calculated, which are not as affected by differences in intensities between the channels as the Pearson coefficient. After deconvolution and background subtraction, Manders coefficients were calculated using the JACoP plugin of ImageJ software.[60] Manders coefficient varies between 0 and 1, where M = 0 represents the lack of colocalization, while complete colocalization is denoted by M = 1.[61,62] Manders colocalization coefficient has two components: $M1$ and $M2$. $M1$ is defined as the ratio of the 'summed intensities of pixels from the green image for which the intensity in the red channel is above zero' to the 'total intensity in the green channel' and $M2$ is defined conversely for the red channel.[63]

RESULTS AND DISCUSSION

Synthesis of the Cholesterol Probe and the Cholesterol Anchor. Our semisynthetic strategy for the preparation of cholesteryl lipoproteins is based on the Michael addition of a C-terminally Cys extended recombinant protein to a maleimide functionalized anchor. Cholesterol was chosen as the lipid moiety of the anchor, because it presumably directs the membrane anchored protein to cholesterol-rich membrane microdomains where GPI-APs are also accumulated. The headgroup of the anchor molecule was designed to be similar in length to the glycan part of the GPIs, and to be able to expose the attached protein to the extracellular space with a distance of ca. 20 Å from the surface of the membrane bilayer (Figure S1). A di(ethylene glycol) spacer between the cholesterol hemisuccinate moiety and the trifunctional linker glycine derivative provides hydrogen bond acceptor ether oxygens that improve the hydrophilic character of the headgoup. Furthermore, the conformational flexibility of this type of spacer is expected to be highly similar to that of the GPI glycan core. It is of interest to note that an endocytosis-inhibiting effect has been reported for cholesteryl ethers with long PEG_{50} and PEG_{200} chains.[64] The cholesterol moiety is attached via an ester bond to the headgroup of the anchor. The hydrolytic stability of this cholesteryl ester is crucial for the imaging applications where the membrane anchored protein is to be visualized by the fluorescence of the headgroup of the anchor. In order to investigate the hydrolytic stability and the membrane association properties of the designed cholesterol anchor, the model compound **3** was synthesized and subjected to preliminary experiments. The cholesterol probe **3** was prepared

Scheme 1. Synthesis of the Fluorescent Cholesterol Probe[a]

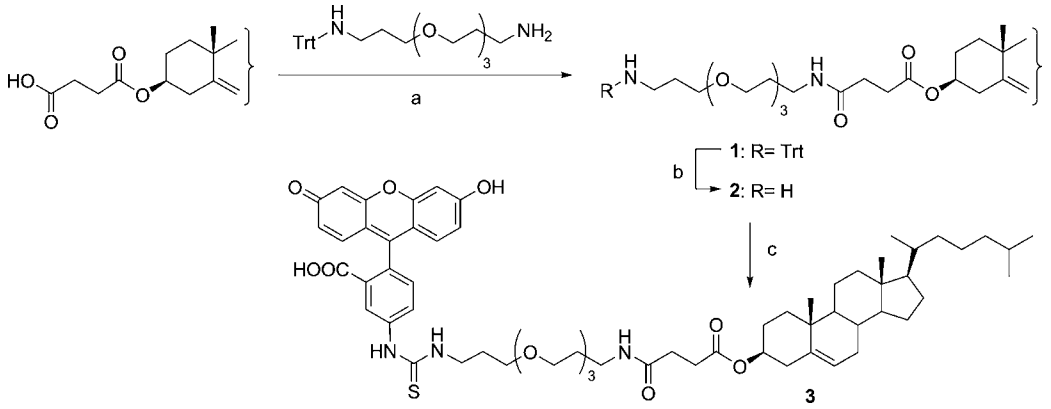

[a](a) 1 equiv TBTU, 1.3 equiv DIEA, $CHCl_3/CH_2Cl_2$ (4:1), RT, 8 h, 95%; (b) TFA, TIS, CH_2Cl_2, RT, 5 × 10 min, 94%; (c) 1.2 equiv FITC, 1 equiv DIEA, DMF, RT, 6 h, 47%.

from cholesteryl hemisuccinate. It was activated with TBTU in the presence of DIEA, and used for the *N*-acylation of the monotrityl protected 1,13-diamino-4,7,10-trioxa-tridecane (Scheme 1). The application of HOBt and DIC resulted in lower yield, and using a dichloromethane/chloroform mixture was also required to achieve a yield of 95% in this acylation step. The trityl group was chosen for protecting the terminal amine, because it is cleaved by mild acids under a condition where the cholesteryl ester is stable. The acidolytic removal of the trityl group of **1** was performed in the presence of triethylsilane that prevented the realkylation of the amine **2** during the deprotection. Finally, the addition of the amine **2** to fluorescein isothiocyanate resulted in the cholesterol probe **3**.

The hydrolytic stability of the cholesteryl ester in **3** was explored by incubating the probe in PBS at ambient temperature, and HPLC analyses were performed at regular time points. It was found that the HPLC peak area of the probe remained constant over a period of 24 h (Figure 1), meaning

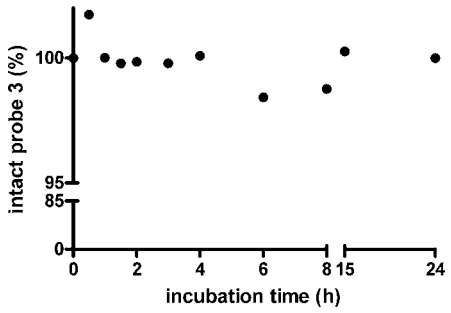

Figure 1. Hydrolytic stability of the cholesterol probe **3**. The peak area of **3** in the incubated sample is indicated as a fraction of the peak area of **3** in the starting solution. Representative chromatograms are shown in Table S2.

that the cholesteryl ester was not hydrolyzed. The chemical stability of the cholesteryl ester is a prerequisite to imaging applications, but the cholesteryl ester also needs to be resistant against cellular esterases. In a subsequent experiment SH-SY5Y cells were treated with 1 μM of **3**, and an intensive membrane staining was observed (Figure 2). These experiments suggested that this cholesteryl ester was stable at physiological pH, and that the hydrophilic headgroup did not prohibit the membrane insertion of the cholesterol amphiphile.

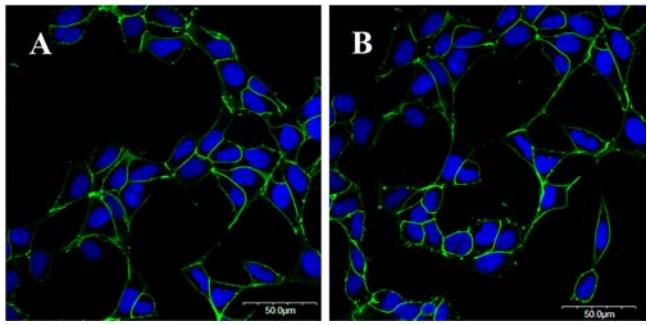

Figure 2. Association of the cholesterol probe **3** (A) and the cholesterol anchor **8** (B) with SH-SY5Y cell membranes. Cells were treated with the compounds at a concentration of 1 μM for 30 min, and nuclear staining was carried out with the nuclear dye DRAQ5 for 5 min. On the image, fluorescein is green and nuclei are blue.

The synthesis of the GPI mimetic cholesterol anchor was conducted in a convergent way (Scheme 2). The synthetic strategy is based on the [3 + 2] cycloaddition of a pegylated azidocholesterol and an alkyne derivative; the latter contains both a thiol reactive maleimide and a fluorescent reporter. The azide−alkyne cycloaddition is fairly fast and chemoselective, and it tolerates the presence of numerous functional groups and a wide range of solvents. Therefore, the demonstrated synthetic strategy can be generally applied for the introduction of diverse fluorescent reporters and protein capture functional groups via the alkyne component, i.e., the headgroup of the cholesterol anchor can be fine-tuned to the experimental setup. The size and the hydrophilic character of the headgroup can be further varied by the introduction of oligo(ethylene glycols) with different length into the azidocholesterol component. The alkyne component was synthesized from propargylglycine (Pra), because the Michael acceptor maleimide and the fluorescent reporter can be orthogonally coupled to the carboxylic and amino groups of Pra without interfering with the alkyne function. The protected maleimido Pra derivative **4** was prepared by the *N*-acylation of *N*-(2-aminoethyl)maleimide with Boc-Pra-OH in the presence of HOBt, DIC, and DIEA. The acidolytic removal of the N^{α}-Boc amino protecting group of **4** resulted in the amine **5**, and the fluorescent alkyne **6** was obtained by the addition of fluorescein isothiocyanate. The alkyne **6** was formed in high yield when **5** was liberated *in situ* from the TFA salt during the isothiocyanate addition. The azide

dx.doi.org/10.1021/bc4002135 | *Bioconjugate Chem.* 2013, 24, 1684−1697

Scheme 2. Synthetic Route to the Green Fluorescent Cholesterol anchor 8[a]

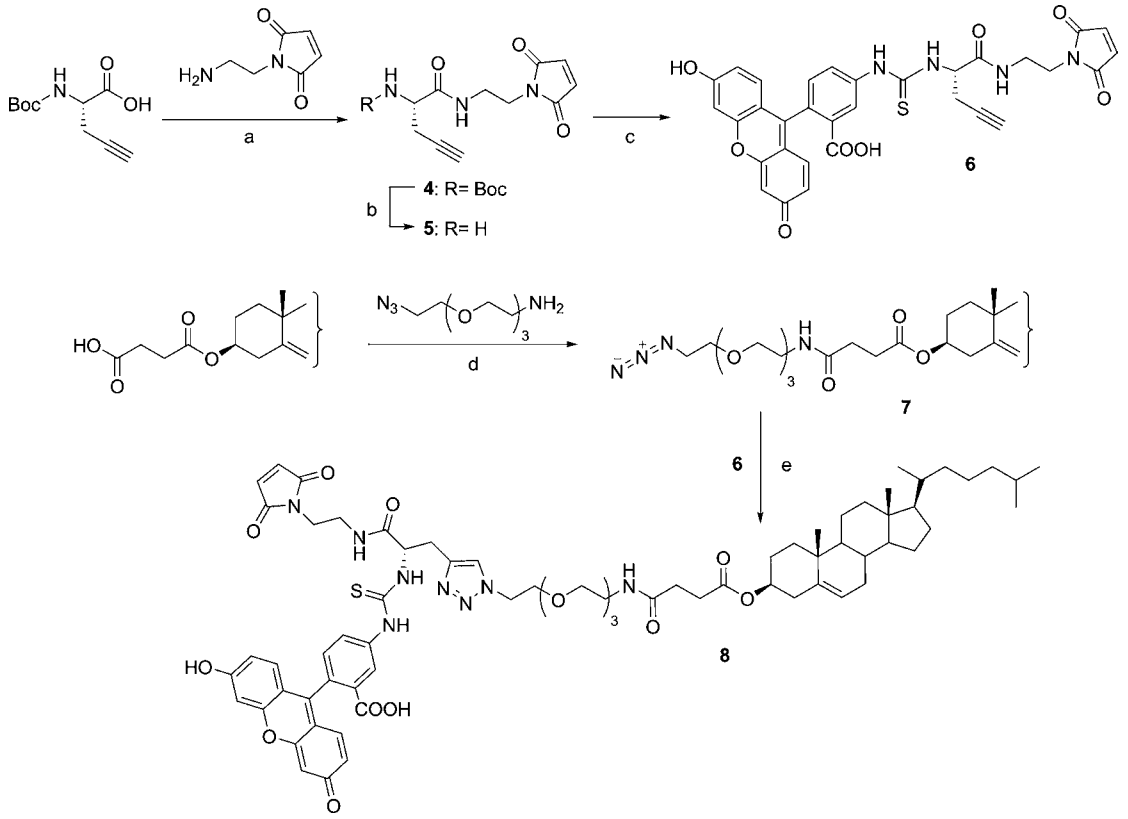

[a](a) 1 equiv HOBt, 1 equiv DIC, 1 equiv DIEA, THF, RT, 8 h, 90%; (b) TFA/CH_2Cl_2 (1:1), RT, 30 min, 96%; (c) 1.05 equiv FITC, 1.05 equiv DIEA, THF, RT, 13 h, 69%; (d) 1.3 equiv TBTU, 1.3 equiv DIEA, $CHCl_3/CH_2Cl_2$ (4:1), RT, 8 h, 90%; (e) 0.6 equiv NaAsc, 0.3 equiv $CuSO_4 \cdot 5H_2O$, *t*BuOH/H_2O (1:1), RT, 48 h, 66%.

component **7** was prepared by the *N*-acylation of 1-amino-11-azido-3,6,9-trioxaundecane with cholesteryl hemisuccinate in the presence of TBTU and DIEA. In the final step the alkyne **6** was linked to the azidolipid **7** by 1,3-dipolar cycloaddition in the presence of $CuSO_4$ and sodium ascorbate in *t*BuOH/H_2O (1:1). The solubility of the resulting cholesterol anchor **8** was investigated in aqueous medium before the protein conjugation and the imaging application. The solution of **8** in serum free medium was incubated at ambient temperature for 16 h, and precipitation was not observed. Then SH-SY5Y cells were treated with 1 μM of **8**, and an intensive membrane staining was obtained (Figure 2). Significant loss of the membrane fluorescence was not observed even 1−3 h after the treatment with **8**, suggesting that the enzymatic cleavage of the headgroup is negligible under our experimental conditions. Beyond an efficient cell membrane association, the lack of cytotoxicity is also an important issue in live cell applications. Therefore the *in vitro* cytotoxic effect of the anchor was also investigated in a subsequent MTT-assay. It was found that the fluorescent cholesterol anchor did not exhibit apparent cytotoxicity after 1 h treatment in the concentration range of 0.26 nM − 100 μM.

Molecular Dynamics Simulations. The atomic details of the association of the cholesterol anchor **8** with DOPC membrane was investigated by MD simulations. This membrane model is a simplified representation of the cell membrane that contains a vast variety of lipids and ca. 30% proteins. However, it represents an electrostatic environment similar to that of the biological membranes, and it is suitable for studying the association mechanism and the atomic orientation of the inserted anchor molecule. First, the simulation system was validated by comparing experimental and calculated characteristic data of the model DOPC bilayer. Good agreement was found between the experimental[65−67] and the calculated values of area per lipid headgroup, bilayer thickness, lateral diffusion coefficient, and deuterium order parameters (Table S3, Figure S2), which confirmed that the applied MD simulation conditions preserved the integrity of the model DOPC bilayer. Two initial setups were created for the production MD: **8** was initially embedded in the DOPC membrane or **8** was initially in the aqueous phase. In the first case, **8** stayed embedded during a 200 ns simulation without visible lateral diffusion. This observation is in agreement with that the time scale of lateral diffusion was reported to be in the range of microseconds.[68] The angle between the membrane plane normal and the vector connecting the 3β-oxygen and C-20 atoms of the cholesterol moiety was found to vary between 0° and 75°, and the distance between C-α and 3β-oxygen varied between 8 Å and 19 Å indicating vigorous axial diffusion and wobbling of the cholesterol moiety of the anchor (Figure 3). In spite of these fast and constant, nanosecond time scale movements, the anchor molecule acquired a relatively stable conformation and arrangement. The conformational change of **8** took place after approximately 20 ns of simulation time and resulted in a special twice-bent shape, which remained relatively stable until the end of the simulation (Figure 4). In this arrangement the di(ethylene glycol) linker lies parallel to the membrane plane, the polar groups of this moiety are in close contact with the lipid headgroups, the cholesterol scaffold is

dx.doi.org/10.1021/bc4002135 | *Bioconjugate Chem.* 2013, 24, 1684−1697

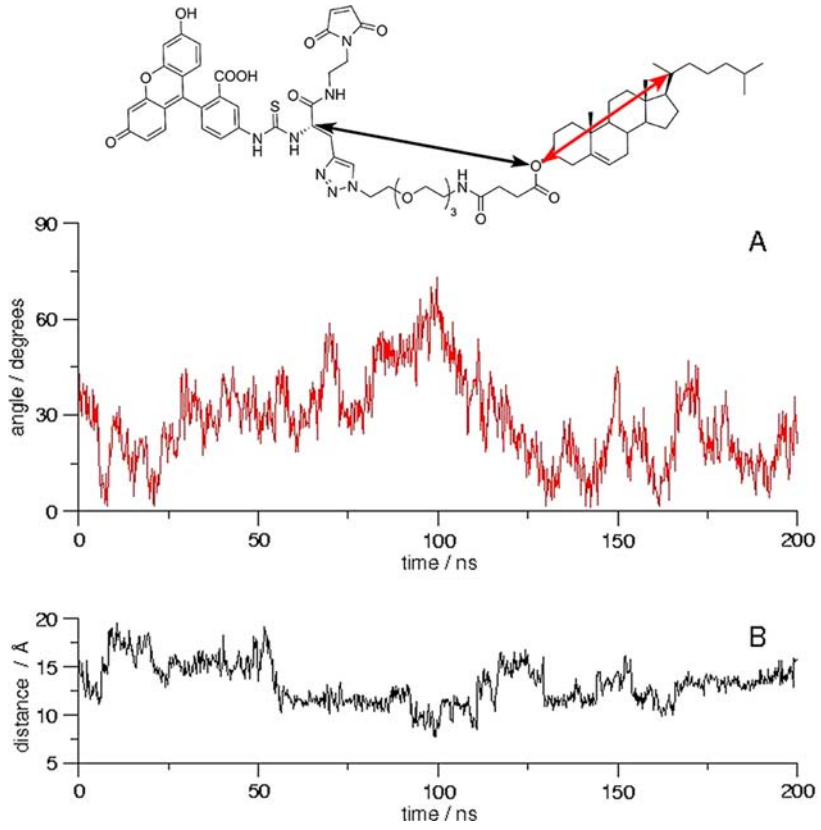

Figure 3. Fluctuation of (A) the angle between the membrane plane normal and the vector connecting the 3β-oxygen and C-20 atoms of the cholesterol moiety (red arrow), and (B) the distance between C-α and 3β-oxygen of anchor **8** (black arrow) during MD simulations.

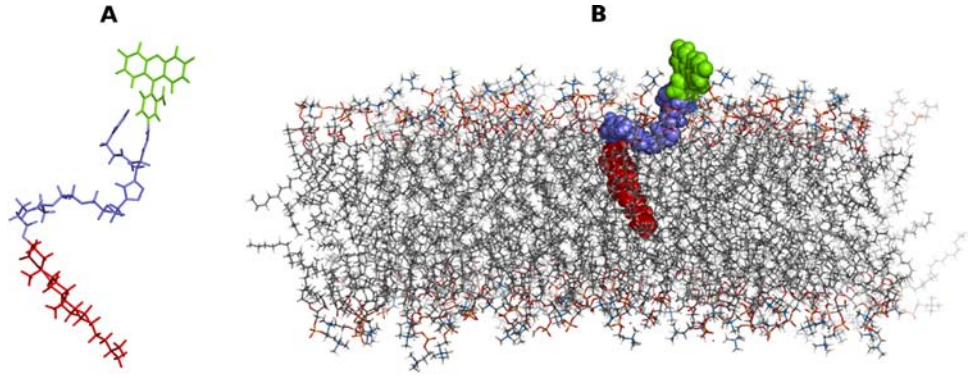

Figure 4. Structure of the cholesterol anchor **8** embedded in DOPC model membrane; water and lipid molecules (A) or just water molecules (B) are omitted for clarity.

immersed in the lipophilic region of the bilayer, and both the maleimido and the fluorescent reporter moieties of the headgroup float in the aqueous phase or form interactions with the DOPC headgroups.

In the second simulation **8** was initially placed in the aqueous phase, and association of the anchor molecule with the membrane surface was observed (Figure S3). While floating in the aqueous phase, **8** adopted a doubled up bent structure, in which the aromatic rings of fluorescein are packed against the cholesterol scaffold to minimize the solvent accessible hydrophobic surface. Membrane association was initiated by polar interactions between the exposed di(ethylene glycol) linker of **8** and the lipid headgroups, observed shortly after 100 ns of simulation time. This initial association then led to the break-up of the intramolecular hydrophobic interactions of **8** and subsequently to the gradual immersion of the cholesterol moiety into the DOPC leaflet. Although this anchor–membrane complex remained stable for the rest of the simulation time, formation of the twice-bent conformation of **8** identified in the first MD simulation was not observed here. It suggests that the spontaneous membrane association and complete membrane embedding of **8** would take longer than 200 ns. It has to be mentioned that simulations presented here were performed for an isolated cholesterol anchor molecule, while **8** forms either micelles or β-cyclodextrin inclusion complexes under the experimental conditions. Therefore, the molecular mechanism of membrane embedding may be different from that described above. Nevertheless, the results of the MD simulations are consistent with the experimental observations of the stable and spontaneous membrane

dx.doi.org/10.1021/bc4002135 | *Bioconjugate Chem.* 2013, 24, 1684–1697

association of **8**. Furthermore, atomic level information was provided about the arrangement of the membrane−anchor complex suggesting that, similarly to the GPI auxiliary, **8** could expose the attached protein toward the aqueous phase while firmly attaching it to the membrane surface.

Protein Conjugation of the Cholesterol Anchor. The red fluorescent protein mCherry lacking any native Cys residues was chosen to optimize the protein−cholesterol anchor conjugation, and to demonstrate that the designed fluorescent cholesterol derivative can anchor proteins to the cell membrane. The C-terminal Cys extension of mCherry resulted in a protein that possessed a single Michael donor thiol group assuring the chemoselective addition of the anchor **8** to the protein C-terminus. A further advantage of this two-color fluorescent lipoprotein conjugate (mCherry − red, fluorescein − green) is that its integrity, i.e., the equimolarity of the protein and the anchor, can easily be assessed by SDS-PAGE and by measuring the intensity of the fluorescence emissions.

mCherry was overexpressed in *E. coli* with a His_6 tag preceding the C-terminal Cys residue, and it was purified from the soluble fraction of the *E. coli* lysate by Ni-affinity chromatography. The conjugation of the cholesterol anchor **8** to mCherry-Cys was performed in 20 mM Tris, 10 mM TCEP at pH 7.5. Under these conditions the β-barrel structure of the protein remains intact, and the amphiphilic cholesterol anchor forms highly stable micellar associates with an approximate critical micellar concentration of 10−100 nM as estimated from data on similar amphiphiles.[55] It was found that the total conversion of mCherry required 25-fold excess of anchor **8** in 1 h (Figure 5). This ratio suggests that the micelles of **8** compose

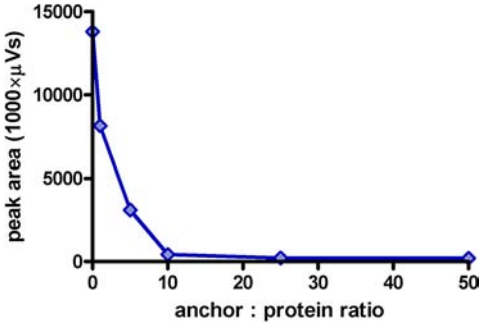

Figure 5. Conjugation of the cholesterol anchor **8** with mCherry-Cys. The concentration of the unreacted mCherry in the reaction mixture after 1 h is indicated (◇).

of ca. 25 cholesterol amphiphiles, and also that a micelle reacts with a single protein molecule. On preparative scale a protein to anchor ratio of 1:10 was applied, and the total amount of **8** was added in 10 portions over 5 h. After the Michael addition, the mixed micelles of the cholesteryl mCherry conjugate and the anchor **8** amphiphiles were separated from both the unreacted protein and the anchor **8** micelles by gel chromatography. According to the elution time, the micellar associates of this cholesteryl mCherry preparation exhibited a virtual molecular weight significantly higher than that of the mCherry (Figure S5). The gel chromatographic fraction containing the mCherry−anchor **8** conjugate was subjected to SDS-PAGE, and an intensive fluorescence was detected in the dye front indicating the presence of mixed micelles. These mixed micellar associates keep the cholesteryl lipoprotein dissolved in an aqueous medium. Nevertheless, it is essential to remove the surplus fluorescent cholesterol; otherwise, the plasma membrane or the cholesterol homeostasis[69] could be perturbed during live cell imaging applications. Furthermore, if the mixed micelles of the conjugate are used for the introduction of the lipoprotein into the cell membrane, the unambiguous imaging of the membrane anchored protein will be impossible via the fluorescence of the cholesterol anchor.

Purification of the Cholesteryl Lipoprotein. Different methods were explored for the separation of the cholesteryl lipoprotein from the surplus fluorescent cholesterol anchor with an emphasis on the retention of the native fold of the protein. Dialysis is commonly used to remove small molecules or lipid excess from protein samples; however, the stability of the mixed micelles of **8** and cholesteryl mCherry limits the performance of this technique. Extraction of the surplus cholesterol anchor with polar solvents is another option, but the application of chloroform denatured the protein. Refolding of such a denatured cholesteryl lipoprotein was not feasible, because the cholesterol residue permanently participates in hydrophobic interactions, and thus, restricts the protein folding. On the other hand, the application of detergents results in mixed detergent micelles of the cholesteryl lipoprotein which are free of surplus fluorescent cholesterol anchors. The introduction of the cholesteryl lipoprotein into the cell membrane via such detergent micelles makes the imaging of the membrane associated protein feasible, but the detergent molecules have a membrane perturbing effect that is to be avoided. When the mixed micelles of mCherry−anchor **8** were purified by reversed phase HPLC, the mixed micelles were disrupted at an acetonitrile concentration of 50% and the cholesteryl mCherry was eluted as a pure semisynthetic product. However, the resulting lipoprotein lost the red fluorescent properties indicating the distortion of the β-barrel structure of mCherry. Afterward, the refolding of this denatured cholesteryl mCherry failed similarly to that of the chloroform extracted cholesteryl mCherry. The application of an anchor capture resin was also intended for the separation of the lipoprotein and the anchor excess by filtering off the resin bound anchor. A cysteinyl CLEAR-amide resin was prepared for that purpose, because it has beneficial water swelling properties. But the heterogeneous Michael addition was found to be very slow, and the mixed micelles remained intact. Finally, another approach was tried, where the cholesterol moiety of the protein−anchor conjugate was sequestered by a reversible complexation with β-cyclodextrin. It is based on the fact that β-cyclodextrin forms a stable inclusion complex with cholesterol.[70] In the presence of low concentration of β-cyclodextrin, cholesterol can be incorporated into the plasma membrane within a few minutes,[71] because the exchange rate of cholesterol between β-cyclodextrin and membranes is high. Furthermore, β-cyclodextrin does not accelerate the extraction of phospholipids from the cell membrane when the concentration of β-cyclodextrin is below 20 mM.[72] When the mixed micelles composed of the cholesteryl mCherry and anchor **8** were incubated with 10 equiv β-cyclodextrin, the micellar associates were disrupted without any sign of denaturing the protein (Figure 6). The hydrophobic cavity of the β-cyclodextrin binds the cholesterol moiety of the conjugate and that of the surplus anchor molecules forming host−guest complexes. The molecular weight of the inclusion complex of the protein−anchor **8** conjugate is significantly higher than that of the cholesterol anchor, and thus, their separation was achieved by size-exclusion chromatography. The purified inclusion complex

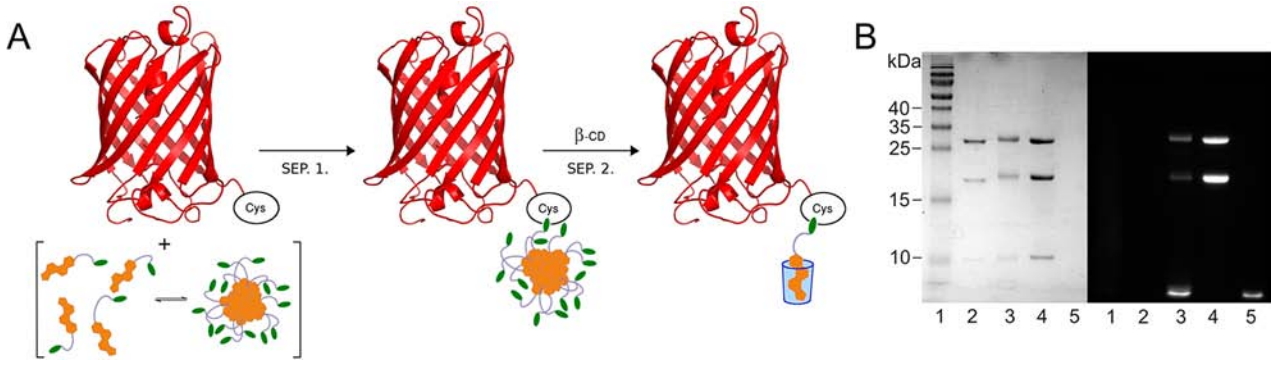

Figure 6. (A) Preparation of the lipid excess-free cholesteryl mCherry. The schematic green heads represent the green fluorophore of the cholesterol anchor **8**; β-cyclodextrin is symbolized with a blue truncated cone; SEP.1. and SEP.2. indicate gel chromatographic separations. (B) Coomassie blue-stained (left) and fluorescence detected (right) 15% SDS-PAGE gel: lane 1, molecular weight marker; lane 2, mCherry (see Scheme S1 for the hydrolysis of the red fluorophore resulting in the multiple band pattern); lane 3, mixed micelles of cholesteryl mCherry (the cholesteryl derivatives of the full length mCherry and the C-terminal mCherry fragment, and the surplus **8** are fluorescent); lane 4, β-cyclodextrin inclusion complex of cholesteryl mCherry (in order to emphasize the lack of surplus anchor **8**, a larger amount of lipoprotein was introduced than in lane 3); lane 5, cholesterol anchor **8**. Quantitation of the fluorescent signals on lanes 3 and 4 was carried out and the ratio of the protein associated fluorescence to the fluorescence of the residual cholesterol anchor is given in Table S4.

of the lipoprotein was subjected to SDS-PAGE analysis followed by fluorescence detection. The intensity of the fluorescent bands of the samples containing the mixed micelles of cholesteryl mCherry and the β-cyclodextrin inclusion complex of cholesteryl mCherry was measured, and the ratio of the protein associated fluorescence to the cholesterol anchor fluorescence was determined using the gel analyzing tool of ImageJ software.[60] The ratio of the intensity of the 27.6 kDa band to the front was found to be 1:2.57 and 1:0.003 before and after the purification via the β-cyclodextrin inclusion complex, respectively (Table S4). Thus, the fluorescence detection revealed that the mCherry–anchor **8** preparation was free of surplus fluorescent anchor.

Characterization of the Cholesteryl Lipoprotein. The fluorescence spectra of the pure lipoprotein exhibited the characteristics of both fluorophores with shoulders on the emission spectrum of fluorescein and on the excitation spectrum of mCherry (Figure 7). The emission spectrum of the red fluorophore was also recorded at an excitation wavelength of 543 nm, because it was applied during the confocal laser scanning microscopic experiments. The red fluorescence of the β-cyclodextrin inclusion complex of cholesteryl mCherry was indicative of the retention of the native protein fold, but it was further evidenced by ECD spectroscopy. Figure 8 shows the ECD spectra of mCherry–Cys and those of the mCherry–anchor **8** conjugate. The fractions of the secondary structural elements of the proteins were calculated by deconvoluting these ECD spectra (Table 1). An almost identical distribution of the helix, β-sheet, turn, and random structures was found for the conjugate and the parent mCherry–Cys. It indicates that the attachment of the cholesterol anchor does not cause significant change in the protein structure, and that the β-barrel fold of mCherry is intact both in the mixed micellar form and in the β-cyclodextrin inclusion complex. The distribution of the secondary structural elements was also calculated from the X-ray diffraction structure of mCherry for comparison. The crystal structure was analyzed with both the DSSP[73] and STRIDE[74] secondary structure recognition algorithms, which yielded very similar results. However, in the solution structures of mCherry–Cys and the mCherry–anchor **8** conjugate, slightly higher fractions

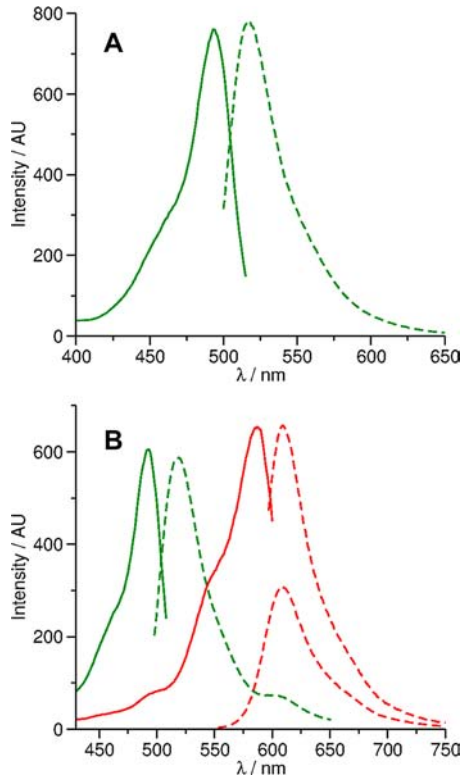

Figure 7. (A) Excitation (—) and emission (- - -) spectra of the cholesterol anchor **8** (50 μM in H_2O) at 25 °C; λ_{em} = 525 nm and λ_{ex} = 488 nm. (B) Excitation (green —, λ_{em} = 518 nm; red —, λ_{em} = 610 nm) and emission (green - - -, λ_{ex}= 488 nm; red - - -, λ_{ex}= 543 and 587 nm) spectra of cholesteryl mCherry (20 μM in H_2O) at 25 °C.

of random structures and lower fractions of β-strands were found. It could be attributed to the flexible N- and C-terminal regions of mCherry that are missing from the X-ray crystal structure.

Imaging of the Cholesteryl Lipoprotein with Confocal Laser Scanning Microscopy. It was shown that our approach offers an effective way to prepare fluorescent cholesteryl lipoproteins without denaturing the protein fold. The integrity of the resulting fluorescent cholesteryl lipoprotein provides the

dx.doi.org/10.1021/bc4002135 | Bioconjugate Chem. 2013, 24, 1684–1697

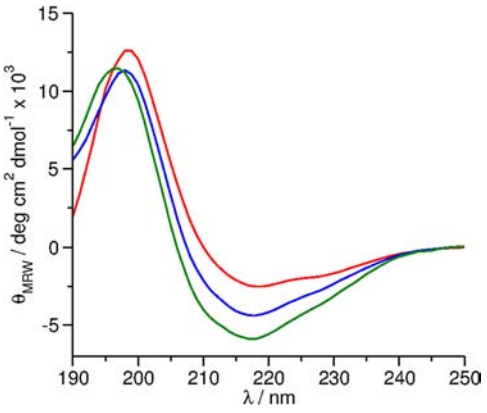

Figure 8. ECD spectra of mCherry-Cys (red), mixed micelles of cholesteryl mCherry (blue), and the β-cyclodextrin inclusion complex of cholesteryl mCherry (green).

Table 1. Fractions of Secondary Structure Elements in mCherry

protein	helix	β-sheet	turns	random
mCherry[a]	0.06	0.57	0.16	0.14
mCherry[b]	0.05	0.58	0.27	0.11
mCherry–Cys[c]	0.09	0.40	0.24	0.27
mCherry–anchor **8** conjugate[c]	0.05	0.43	0.24	0.28
mCherry–anchor **8** conjugate with β-CD[c]	0.07	0.41	0.25	0.26

[a]Results obtained from PDB 2H5Q by DSSP algorithm. [b]Results obtained from PDB 2H5Q by STRIDE algorithm. [c]Results obtained from experimental ECD spectra by deconvolution.

advantage of avoiding the coadministration of surplus, non-conjugated fluorescent lipids and detergents, and thus, the membrane perturbation by external lipid excess or detergents can be excluded in live cell imaging applications. Importantly, the fluorescence signal of the anchor molecule can be unambiguously assigned to the conjugated protein. In order to introduce the semisynthetic lipoprotein into the plasma membrane of live cells, the mCherry–anchor **8** conjugate was added to a mammalian cell culture along with controls (anchor **8** or mCherry–Cys alone) and monitored by confocal laser scanning microscopy. Images of SH-SY5Y cells incubated with the β-cyclodextrin inclusion complex of the semisynthetic mCherry–anchor **8** conjugate show green and red fluorescence on the cell membrane (Figure 9). This suggests that the protein is successfully anchored to the cell membrane after exogenous addition, and also that the protein structure is not affected by the membrane association. Red fluorescence was not observed when cells were treated with mCherry–Cys, confirming that the cholesteryl lipoprotein was firmly associated to the cell membrane via the cholesterol anchor. The membrane association of the conjugate also results in the liberation of β-cyclodextrin from the inclusion complex. However, the presence of 10–20 μM β-cyclodextrin in the cell culture medium has no effect on the normal cellular cholesterol level, because the cholesterol extraction from the cell membrane requires higher β-cyclodextrin concentration in the mM range.[75] It is important to note that, due to the structure of the anchor and the moderate hydrophobicity of fluorescein, the fluorescent reporter is expected to be situated extracellularly. It is in agreement with the results of the MD simulations on the anchor **8**, where only the cholesterol residue immersed into the outer leaflet of the membrane bilayer. This spatial arrangement of the conjugate helps to maintain lipid–lipid interactions specific for cholesterol, and proposes lateral diffusion properties similar to that of cholesterol. These membrane biophysical properties would be altered if the sterane skeleton was modified with a fluorescent molecule.[76] The colocalization of the fluorophores also evidenced that the cholesteryl ester and consequently the whole conjugate was stable under the circumstances of the live cell imaging. In order to quantitate the colocalization of the mCherry and fluorescein fluorophores, the Manders colocalization coefficients were calculated. The original $M1$ and $M2$ values were found to be 0.993 ± 0.020 and 0.999 ± 0.001, respectively. These data represent high colocalization, which is unambiguously visualized in Figure 9B. It is also visible on the differential interference contrast picture that the conjugate exhibited no apparent toxic effects on the SH-SY5Y cells. This finding is in agreement with the results

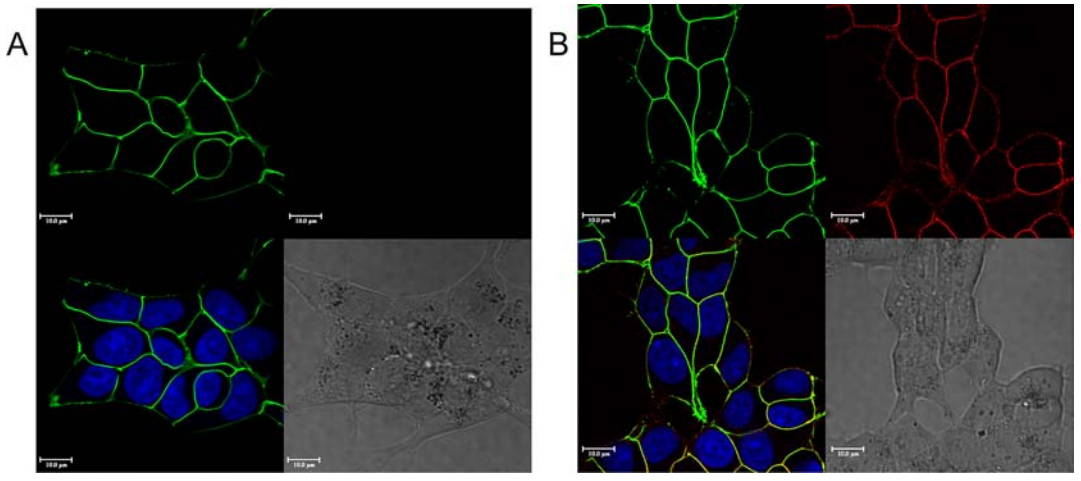

Figure 9. Confocal laser scanning and differential interference contrast (right bottom) microscopy of SH-SY5Y cells after 30 min incubation (A) with 1 μM cholesterol anchor **8**, and (B) with β-cyclodextrin inclusion complex of 1 μM cholesteryl mCherry at 37 °C. On the images fluorescein is green, mCherry is red, and nuclei are blue. On the overlaid image (A and B, left bottom) yellow represents the colocalization of the fluorescein and mCherry signals.

dx.doi.org/10.1021/bc4002135 | Bioconjugate Chem. 2013, 24, 1684–1697

of the MTT assays, where the mCherry−anchor **8** conjugate was found to be nontoxic at a concentration of 10 μM.

CONCLUSIONS

A general approach for the modification of proteins with fluorescent cholesterol derivatives is suggested, where the resulting semisynthetic proteins enable the direct imaging of membrane associated cholesteryl proteins after exogenous introduction into live cells. The appropriate cholesterol anchor is prepared with a convergent synthetic strategy that allows flexibility in the molecular design of the headgroup, i.e., the Michael acceptor, the length of the PEG spacer, and the fluorescent reporter molecule all can be fine-tuned to the preferences of the particular application, to the target protein, and to the instrumentation. The stable membrane association of the cholesterol anchor was confirmed experimentally, and an extracellular orientation of the headgroup is in agreement with the molecular dynamics simulations performed with anchor **8**. As a proof of concept, the method was demonstrated on the red fluorescent protein mCherry that was conjugated with a green fluorescent anchor. Due to the presence and position of the green fluorescent reporter, the purity and the homogeneity of the cholesteryl lipoprotein could be unambiguously analyzed. Furthermore, the retention of the red fluorescence of mCherry was indicative of the preservation of the native protein fold after cholesterol conjugation, and after delivery into membranes of live cells. In imaging applications, the model protein mCherry can be substituted with other target proteins having a C-terminal Cys residue. The main advantage of our method is that the use of the β-cyclodextrin inclusion complex of the protein conjugate allows the treatment of live cells with fluorescent cholesteryl lipoproteins without the use of membrane perturbing detergents. Furthermore, no surplus fluorescent lipids over the stoichiometric cholesterol moiety of the semisynthetic lipoprotein are introduced into the cell membrane. As a consequence, direct imaging of a membrane anchored protein became feasible with a small molecule fluorophore, and thus, the strategy offers a beneficial alternative to GFP fusions for studying membrane associated proteins. Our conjugation method might also be applied in fluorescence microscopic investigation of the cellular traffic of GPI-APs and in cell surface engineering, because the exogenous insertion of pure cholesteryl lipoproteins into cell membranes causes a lower degree of stress to the recipient cells as compared to the liposome fusion or micelle fusion methods.

ASSOCIATED CONTENT

Supporting Information

Comparison of a GPI anchor and the designed cholesterol anchor; synthetic procedures, numbering of compounds for NMR assignation; representative RP-HPLC chromatograms; details of the MD simulations; MD simulation snapshots of the membrane association of **8**; plasmid construction for mCherry-Cys. This material is available free of charge via the Internet at http://pubs.acs.org.

AUTHOR INFORMATION

Corresponding Author

*E-mail: tomboly@brc.hu. Phone: +36-62-599-646. Fax: +36-62-433-506.

Present Address

Erika Orbán, Institute of Biophysical Chemistry, Goethe University Frankfurt, Max-von-Laue str. 9, 60438 Frankfurt, Germany.

Notes

The authors declare no competing financial interest.

ACKNOWLEDGMENTS

Financial support from the Hungarian Scientific Research Fund (K77783 (Cs.T.) and K82090 (E.W.)), from the Hungarian National Development Agency (TÁMOP 4.2.2.A-11/1/KONV-2012-0052 (Cs.T.) and TÁMOP 4.2.4.A/2-11-1-2012-0001 (A.B.), and the János Bolyai Research Scholarship of the Hungarian Academy of Sciences (Cs.T.), and access granted to the high performance computing centre of the National Information Infrastructure Development Institute (A.B.) are acknowledged. We also thank D. Tourwé for critical reading of the manuscript and helpful discussions.

REFERENCES

(1) Hang, H. C., Wilson, J. P., and Charron, G. (2011) Bioorthogonal chemical reporters for analyzing protein lipidation and lipid trafficking. *Acc. Chem. Res. 44*, 699−708.

(2) Gordon, J. I., Duronio, R. J., Rudnick, D. A., Adams, S. P., and Gokel, G. W. (1991) Protein N-myristoylation. *J. Biol. Chem. 266*, 8647−8650.

(3) Smotrys, J. E., and Linder, M. E. (2004) Palmitoylation of intracellular signaling proteins: regulation and function. *Annu. Rev. Biochem. 73*, 559−587.

(4) Towler, D. A., Gordon, J. I., Adams, S. P., and Glaser, L. (1988) The biology and enzymology of eukaryotic protein acylation. *Annu. Rev. Biochem. 57*, 69−99.

(5) Fu, H. W., and Casey, P. J. (1999) Enzymology and biology of CaaX protein prenylation. *Recent Prog. Horm. Res. 54*, 315−342.

(6) Low, M. G. (1989) The glycosyl-phosphatidylinositol anchor of membrane-proteins. *Biochim. Biophys. Acta 988*, 427−454.

(7) Low, M. G., and Saltiel, A. R. (1988) Structural and functional roles of glycosyl-phosphatidylinositol in membranes. *Science 239*, 268−275.

(8) Englund, P. T. (1993) The structure and biosynthesis of glycosyl phosphatidylinositol protein anchors. *Annu. Rev. Biochem. 62*, 121−138.

(9) Paulick, M. G., and Bertozzi, C. R. (2008) The glycosylphosphatidylinositol anchor: a complex membrane-anchoring structure for proteins. *Biochemistry 47*, 6991−7000.

(10) Kinoshita, T. and Fujita, M. (2009) Overview of GPI biosynthesis. *The Enzymes. Vol. 26: Glycosylphosphatidylinositol (GPI) anchoring of proteins* (Menon, A. K., Kinoshita, T., Orlean, P., Tamanoi, F., Eds.) pp 1−30, Academic Press, New York.

(11) Savage, V. J., and Brodsky, R. A. (2006) New insights into paroxysmal nocturnal hemoglobinuria. *Hematology 12*, 371−376.

(12) Prusiner, S. B. (1998) Prions. *Proc. Natl. Acad. Sci. U. S. A. 95*, 13363−13383.

(13) Zhao, P., Nairn, A. V., Hester, S., Moremen, K. W., O'Regan, R. M., Oprea, G., Wells, L., Pierce, M., and Abbott, K. L. (2012) Proteomic identification of glycosylphosphatidylinositol anchor-dependent membrane proteins elevated in breast carcinoma. *J. Biol. Chem. 287*, 25230−25240.

(14) Ferguson, M. A. (1999) The structure, biosynthesis and functions of glycosylphosphatidylinositol anchors, and the contributions of trypanosome research. *J. Cell Sci. 112*, 2799−2809.

(15) Nozaki, M., Ohishi, K., Yamada, N., Kinoshita, T., Nagy, A., and Takeda, J. (1999) Developmental abnormalities of glycosylphosphatidylinositol-anchor-deficient embryos revealed by Cre/loxP system. *Lab. Invest. 79*, 293−299.

(16) Chatterjee, S., and Mayor, S. (2001) The GPI-anchor and protein sorting. *Cell. Mol. Life Sci. 58*, 1969−1987.

(17) Low, M. G. (1989) Glycosyl-phosphatidylinositol: a versatile anchor for cell surface proteins. *FASEB J. 3*, 1600−1608.
(18) Mayor, S., and Riezman, H. (2004) Sorting GPI-anchored proteins. *Nat. Rev. Mol. Cell Biol. 5*, 110−120.
(19) Eggeling, C., Ringemann, C., Medda, R., Schwarzmann, G., Sandhoff, K., Polyakova, S., Belov, V. N., Hein, B., von Middendorff, C., Schonle, A., and Hell, S. W. (2009) Direct observation of the nanoscale dynamics of membrane lipids in a living cell. *Nature 457*, 1159−1162.
(20) Simons, K., and Gerl, M. J. (2010) Revitalizing membrane rafts: new tools and insights. *Nat. Rev. Mol. Cell Biol. 11*, 688−699.
(21) Lingwood, D., and Simons, K. (2010) Lipid rafts as a membrane-organizing principle. *Science 327*, 46−50.
(22) Sharma, P., Varma, R., Sarasij, R. C., Ira, Gousset, K., Krishnamoorthy, G., Rao, M., and Mayor, S. (2004) Nanoscale organization of multiple GPI-anchored proteins in living cell membranes. *Cell 116*, 577−589.
(23) Simons, K., and Ikonen, E. (1997) Functional rafts in cell membranes. *Nature 387*, 569−572.
(24) Simons, K., and Toomre, D. (2000) Lipid rafts and signal transduction. *Nat. Rev. Mol. Cell Biol. 1*, 31−39.
(25) Ball, H. L., King, D. S., Cohen, F. E., Prusiner, S. B., and Baldwin, M. A. (2001) Engineering the prion protein using chemical synthesis. *J. Pept. Res. 58*, 357−374.
(26) Eberl, H., Tittmann, P., and Glockshuber, R. (2004) Characterization of recombinant, membrane-attached full-length prion protein. *J. Biol. Chem. 279*, 25058−25065.
(27) Musiol, H. J., Dong, S., Kaiser, M., Bausinger, R., Zumbusch, A., Bertsch, U., and Moroder, L. (2005) Toward semisynthetic lipoproteins by convergent strategies based on click and ligation chemistry. *ChemBioChem 6*, 625−628.
(28) Grogan, M. J., Kaizuka, Y., Conrad, R. M., Groves, J. T., and Bertozzi, C. R. (2005) Synthesis of lipidated green fluorescent protein and its incorporation in supported lipid bilayers. *J. Am. Chem. Soc. 127*, 14383−14387.
(29) Paulick, M. G., Wise, A. R., Forstner, M. B., Groves, J. T., and Bertozzi, C. R. (2007) Synthetic analogues of glycosylphosphatidylinositol-anchored proteins and their behavior in supported lipid bilayers. *J. Am. Chem. Soc. 129*, 11543−11550.
(30) Hicks, M. R., Gill, A. C., Bath, I. K., Rullay, A. K., Sylvester, I. D., Crout, D. H., and Pinheiro, T. J. (2006) Synthesis and structural characterization of a mimetic membrane-anchored prion protein. *FEBS J. 273*, 1285−1299.
(31) Breydo, L., Sun, Y., Makarava, N., Lee, C. I., Novitskaia, V., Bocharova, O., Kao, J. P., and Baskakov, I. V. (2007) Nonpolar substitution at the C-terminus of the prion protein, a mimic of the glycosylphosphatidylinositol anchor, partially impairs amyloid fibril formation. *Biochemistry 46*, 852−861.
(32) Olschewski, D., Seidel, R., Miesbauer, M., Rambold, A. S., Oesterhelt, D., Winklhofer, K. F., Tatzelt, J., Engelhard, M., and Becker, C. F. (2007) Semisynthetic murine prion protein equipped with a GPI anchor mimic incorporates into cellular membranes. *Chem. Biol. 14*, 994−1006.
(33) Becker, C. F., Liu, X., Olschewski, D., Castelli, R., Seidel, R., and Seeberger, P. H. (2008) Semisynthesis of a glycosylphosphatidylinositol-anchored prion protein. *Angew. Chem., Int. Ed. 47*, 8215−8219.
(34) Teruya, K., Nishizawa, K., and Doh-ura, K. (2010) Semisynthesis of a protein with cholesterol at the C-terminal, targeted to the cell membrane of live cells. *Protein J. 29*, 493−500.
(35) Paulick, M. G., Forstner, M. B., Groves, J. T., and Bertozzi, C. R. (2007) A chemical approach to unraveling the biological function of the glycosylphosphatidylinositol anchor. *Proc. Natl. Acad. Sci. U. S. A. 104*, 20332−20337.
(36) Medof, M. E., Kinoshita, T., and Nussenzweig, V. (1984) Inhibition of complement activation on the surface of cells after incorporation of decay-accelerating factor (DAF) into their membranes. *J. Exp. Med. 160*, 1558−1578.
(37) van den Berg, C. W., Cinek, T., Hallett, M. B., Horejsi, V., and Morgan, B. P. (1995) Exogenous glycosyl phosphatidylinositol-anchored CD59 associates with kinases in membrane clusters on U937 cells and becomes Ca(2+)-signaling competent. *J. Cell Biol. 131*, 669−677.
(38) Medof, M. E., Nagarajan, S., and Tykocinski, M. L. (1996) Cell-surface engineering with GPI-anchored proteins. *FASEB J. 10*, 574−586.
(39) Premkumar, D. R., Fukuoka, Y., Sevlever, D., Brunschwig, E., Rosenberry, T. L., Tykocinski, M. L., and Medof, M. E. (2001) Properties of exogenously added GPI-anchored proteins following their incorporation into cells. *J. Cell Biochem. 82*, 234−245.
(40) Milhiet, P. E., Giocondi, M. C., Baghdadi, O., Ronzon, F., Roux, B., and Le Grimellec, C. (2002) Spontaneous insertion and partitioning of alkaline phosphatase into model lipid rafts. *EMBO Rep. 3*, 485−490.
(41) Rifkin, M. R., and Landsberger, F. R. (1990) Trypanosome variant surface glycoprotein transfer to target membranes: a model for the pathogenesis of trypanosomiasis. *Proc. Natl. Acad. Sci. U. S. A. 87*, 801−805.
(42) Dunn, D. E., Yu, J., Nagarajan, S., Devetten, M., Weichold, F. F., Medof, M. E., Young, N. S., and Liu, J. M. (1996) A knock-out model of paroxysmal nocturnal hemoglobinuria: Pig-a(-) hematopoiesis is reconstituted following intercellular transfer of GPI-anchored proteins. *Proc. Natl. Acad. Sci. U. S. A. 93*, 7938−7943.
(43) Metzner, C., Mostegl, M. M., Gunzburg, W. H., Salmons, B., and Dangerfield, J. A. (2008) Association of glycosylphosphatidylinositol-anchored protein with retroviral particles. *FASEB J. 22*, 2734−2739.
(44) Metzner, C., Kochan, F., and Dangerfield, J. A. (2013) Fluorescence molecular painting of enveloped viruses. *Mol. Biotechnol. 53*, 9−18.
(45) Porter, J. A., Young, K. E., and Beachy, P. A. (1996) Cholesterol modification of hedgehog signaling proteins in animal development. *Science 274*, 255−259.
(46) Mann, R. K., and Beachy, P. A. (2004) Novel lipid modifications of secreted protein signals. *Annu. Rev. Biochem. 73*, 891−923.
(47) Rietveld, A., Neutz, S., Simons, K., and Eaton, S. (1999) Association of sterol- and glycosylphosphatidylinositol-linked proteins with Drosophila raft lipid microdomains. *J. Biol. Chem. 274*, 12049−12054.
(48) Taipale, J., Chen, J. K., Cooper, M. K., Wang, B., Mann, R. K., Milenkovic, L., Scott, M. P., and Beachy, P. A. (2000) Effects of oncogenic mutations in Smoothened and Patched can be reversed by cyclopamine. *Nature 406*, 1005−1009.
(49) Peters, C., Wolf, A., Wagner, M., Kuhlmann, J., and Waldmann, H. (2004) The cholesterol membrane anchor of the Hedgehog protein confers stable membrane association to lipid-modified proteins. *Proc. Natl. Acad. Sci. U. S. A. 101*, 8531−8536.
(50) Hussey, S. L., He, E., and Peterson, B. R. (2001) A synthetic membrane-anchored antigen efficiently promotes uptake of antifluorescein antibodies and associated protein a by mammalian cells. *J. Am. Chem. Soc. 123*, 12712−12713.
(51) Hussey, S. L., and Peterson, B. R. (2002) Efficient delivery of streptavidin to mammalian cells: clathrin-mediated endocytosis regulated by a synthetic ligand. *J. Am. Chem. Soc. 124*, 6265−6273.
(52) Martin, S. E., and Peterson, B. R. (2003) Non-natural cell surface receptors: synthetic peptides capped with N-cholesterylglycine efficiently deliver proteins into Mammalian cells. *Bioconjugate Chem. 14*, 67−74.
(53) Boonyarattanakalin, S., Martin, S. E., Dykstra, S. A., and Peterson, B. R. (2004) Synthetic mimics of small mammalian cell surface receptors. *J. Am. Chem. Soc. 126*, 16379−16386.
(54) Boonyarattanakalin, S., Martin, S. E., Sun, Q., and Peterson, B. R. (2006) A synthetic mimic of human Fc receptors: defined chemical modification of cell surfaces enables efficient endocytic uptake of human immunoglobulin-G. *J. Am. Chem. Soc. 128*, 11463−11470.
(55) Tomas, S., and Milanesi, L. (2009) Hydrophobically self-assembled nanoparticles as molecular receptors in water. *J. Am. Chem. Soc. 131*, 6618−6623.

(56) Tomas, S., and Milanesi, L. (2010) Mutual modulation between membrane-embedded receptor clustering and ligand binding in lipid membranes. *Nat. Chem. 2*, 1077−1083.
(57) Bradford, M. M. (1976) A rapid and sensitive method for the quantitation of microgram quantities of protein utilizing the principle of protein-dye binding. *Anal. Biochem. 72*, 248−254.
(58) Sreerama, N. and Woody, R. W. (2000) Circular dichroism of peptides and proteins. *Circular Dichroism*, 2nd ed. (Berova, N., Nakanishi, K. and Woody, R. W., Eds.) pp 601−620, John Wiley & Sons, Inc., New York.
(59) Slater, T. F., Sawyer, B., and Straeuli, U. (1963) Studies on succinate-tetrazolium reductase systems. III. Points of coupling of four different tetrazolium salts. *Biochim. Biophys. Acta 77*, 383−393.
(60) http://rsbweb.nih.gov/ij/plugins/track/jacop.html.
(61) Hibbs, A. R., MacDonald, G., and Garsha, K. (2006) Practical confocal microscopy. In *Handbook of biological confocal microscopy* (Pawley, J. B., Ed.) pp 667−670, Chapter 36, Springer, New York.
(62) Adler, J., and Parmryd, I. (2010) Quantifying colocalization by correlation: the Pearson correlation coefficient is superior to the Mander's overlap coefficient. *Cytometry A 77*, 733−742.
(63) Bolte, S., and Cordelieres, F. P. (2006) A guided tour into subcellular colocalization analysis in light microscopy. *J. Microsc. 224*, 213−232.
(64) Sato, S. B., Ishii, K., Makino, A., Iwabuchi, K., Yamaji-Hasegawa, A., Senoh, Y., Nagaoka, I., Sakuraba, H., and Kobayashi, T. (2004) Distribution and transport of cholesterol-rich membrane domains monitored by a membrane-impermeant fluorescent polyethylene glycol-derivatized cholesterol. *J. Biol. Chem. 279*, 23790−23796.
(65) Liu, Y. F., and Nagle, J. F. (2004) Diffuse scattering provides material parameters and electron density profiles of biomembranes. *Phys. Rev. E 69*, 040901.
(66) Filippov, A., Oradd, G., and Lindblom, G. (2003) Influence of cholesterol and water content on phospholipid lateral diffusion in bilayers. *Langmuir 19*, 6397−6400.
(67) Warschawski, D. E., and Devaux, P. F. (2005) Order parameters of unsaturated phospholipids in membranes and the effect of cholesterol: a H-1-C-13 solid-state NMR study at natural abundance. *Eur. Biophys. J. 34*, 987−996.
(68) Vermeer, L. S., de Groot, B. L., Reat, V., Milon, A., and Czaplicki, J. (2007) Acyl chain order parameter profiles in phospholipid bilayers: computation from molecular dynamics simulations and comparison with 2H NMR experiments. *Eur. Biophys. J. 36*, 919−931.
(69) Simons, K., and Ikonen, E. (2000) How cells handle cholesterol. *Science 290*, 1721−1726.
(70) Ravichandran, R., and Divakar, S. (1998) Inclusion of ring A of cholesterol inside the beta-cyclodextrin cavity: Evidence from oxidation reactions and structural studies. *J. Inclusion Phenom. Mol. Recognit. Chem. 30*, 253−270.
(71) Tsamaloukas, A., Szadkowska, H., Slotte, P. J., and Heerklotz, H. (2005) Interactions of cholesterol with lipid membranes and cyclodextrin characterized by calorimetry. *Biophys. J. 89*, 1109−1119.
(72) Niu, S. L., and Litman, B. J. (2002) Determination of membrane cholesterol partition coefficient using a lipid vesicle-cyclodextrin binary system: effect of phospholipid acyl chain unsaturation and headgroup composition. *Biophys. J. 83*, 3408−3415.
(73) Kabsch, W., and Sander, C. (1983) Dictionary of protein secondary structure: pattern recognition of hydrogen-bonded and geometrical features. *Biopolymers 22*, 2577−2637.
(74) Frishman, D., and Argos, P. (1995) Knowledge-based protein secondary structure assignment. *Proteins 23*, 566−579.
(75) Kilsdonk, E. P., Yancey, P. G., Stoudt, G. W., Bangerter, F. W., Johnson, W. J., Phillips, M. C., and Rothblat, G. H. (1995) Cellular cholesterol efflux mediated by cyclodextrins. *J. Biol. Chem. 270*, 17250−17256.
(76) Scheidt, H. A., Muller, P., Herrmann, A., and Huster, D. (2003) The potential of fluorescent and spin-labeled steroid analogs to mimic natural cholesterol. *J. Biol. Chem. 278*, 45563−45569.